Hindawi
Geofluids
Volume 2023, Article ID 2201870, 23 pages
https://doi.org/10.1155/2023/2201870

*Research Article*

# Analytical Model of Wellbore Stability Analysis of Inclined Well Based on the Advantageous Synergy among the Five Strength Criteria

**Yufan Shi**,[1,2] **Tianshou Ma**,[2] **Dongyang Zhang**,[2] **Yingjie Chen**,[3] **Yang Liu**,[4] **and Changsong Deng**[5]

[1]*School of Engineering, Southwest Petroleum University, Nanchong 637001, China*
[2]*State Key Laboratory of Oil and Gas Reservoir Geology and Exploitation, Southwest Petroleum University, Chengdu 610500, China*
[3]*Tight Oil and Gas Project Division, PetroChina Southwest Oil & Gas Field Company, Chengdu 610056, China*
[4]*Cementing Company, Great Wall Drilling Company, CNPC, Panjin 124010, China*
[5]*PetroChina Tarim Oilfield Company, Korla 841000, China*

Correspondence should be addressed to Tianshou Ma; matianshou@126.com

Received 15 August 2022; Revised 17 October 2022; Accepted 28 November 2022; Published 6 February 2023

Academic Editor: Jianchao Cai



The proper drilling mud density is vital for wellbore stability maintenance, which relies on both stress distribution on the borehole wall and rock strength. Thus, the selection of rock strength criterion is vital for wellbore stability analysis (WSA), and several strength criteria have been developed and employed to perform WSA, but the real collapse pressure does not comply with any single strength criterion. Therefore, to accurately predict the critical mud weight against wellbore collapse, an analytical model of WSA was proposed for inclined wells based on the advantageous synergy among the five types of strength criteria, such as the Mohr-Coulomb criterion, Mogi-Coulomb criterion, Drucker-Prager criterion, modified Wiebols-Cook criterion, and modified Lade criterion. The predicted results among these analytical and five conventional models were compared under three kinds of typical stress regimes, such as normal, strike-slip, and reverse faults. Finally, five kinds of typical oil and gas field data were collected to further verify the accuracy of this new model. The results indicated that different models predicted different collapse pressure, owing to the Mohr-Coulomb criterion ignoring the intermediate principal stress ($\sigma_2$), so as to always give the greatest collapse pressure, followed by the present analytical model and the Mogi-Coulomb criterion, while the other three types of strength criteria gave different results, because of the difference in the influence of $\sigma_2$, while the present analytical model integrated the advantageous synergy among the five strength criteria. The prediction error of the conventional analytical model ranges from 9.4 to 34.2% with an average of 22.1%, while the prediction error of this new model ranges from 2.3 to 12.5% with an average of 7.1%, so that the present analytical model has much higher accuracy than that of any single strength criterion. In addition, this new analytical model can be simplified as the conventional analytical model by adjusting the weight coefficients.

## 1. Introduction

In recent years, unconventional petroleum reservoirs are receiving increasing attentions [1], particularly, shale reservoir [2], tight-sand reservoir [3], and coalbed methane reservoir [4]. Owing to advances in directional drilling technologies, directional, horizontal, and extended-reach wells are widely employed to develop these unconventional petroleum reservoirs [5, 6]. Although these types of nonvertical wells, particularly, horizontal wells, are much more expensive than that of vertical wells, they are more popular owing to their advantages in enhancing oil and gas production, lowering surface well pad construction, and lowering comprehensive development cost [7], so they have become very valuable techniques in recent years. However, in the process of drilling such types of inclined wells, the engineers usually

encounter some complicated problems, such as high risk of wellbore instability [8], excessive drill-string drag [9], hole cleaning in highly deviated wellbore [10], and high risk of pipe sticking and casing wear [11], which will cause long nonproductive time, long drilling cycle, and high drilling costs [12, 13]. Among them, wellbore instability is always one of the most difficult problems owing to its costly consequences [14–16]. An inaccurate or improper wellbore stability analysis (WSA) can always cause several serious consequences, particularly wellbore collapse, lost circulation, drill pipe sticking, drill pipe burying, and even borehole abandonment [17–19]. According to incomplete statistics, wellbore instability may cost hundreds of millions of dollars in direct economic losses each year [8, 19–23].

Wellbore instability is mainly caused by excessive stress concentration near the borehole [8, 24]. When a borehole is drilled and formed, the original rock is removed from the formation, so its support effect is replaced by the drilling mud, which will cause stress redistribution near the borehole, and wellbore instability may occur when stress exceeds rock strength. As shown in Figure 1, the mechanical failure of wellbore can be classified as (1) wellbore collapse caused by compressive failure and (2) wellbore fracture caused by tensile failure [25, 26]. Too low mud weight (or drilling fluid density) may cause wellbore breakout and even wellbore collapse, while too high mud weight may cause wellbore fracture and even lost circulation. Therefore, in order to maintain the stability of borehole, the major concerns are to design a proper mud weight and mud formula [19, 27]. Thus, the WSA is vital for designing a proper mud weight to maintain wellbore stability. To accurately predict the collapse and fracture pressures, various analytical and numerical models have been proposed and employed for WSA [8, 15, 19–38], and most of them are still elastic methods. The most common elastic analysis process of wellbore stability includes two major steps [8]: (1) determine the wellbore stress components using analytical solutions of elastic stress distribution and (2) estimate the wellbore failure by selecting a proper strength criterion.

Several studies have indicated that the selection of rock strength criterion is vital for WSA. Bradley [38] employed the Mohr-Coulomb (M-C) criterion to predict collapse pressure of inclined wells, but the M-C criterion ignored the intermediate stress ($\sigma_2$), underestimating rock strength. Ewy [39] recommended to use a modified Lade (ML) criterion to conduct WSA for inclined wells. Colmenares and Zoback [40] examined seven types of strength criteria, the results indicated that both modified Wiebols-Cook (MW-C) and ML are in good agreement with the testing rock strength, and they recommended using these two criteria for WSA. Al-Ajmi and Zimmerman [41] proposed the Mogi-Coulomb (Mg-C) criterion, an empirical strength criterion, and the results showed that the Mg-C can accurately match with the polyaxial strength data, so it is therefore widely applied for WSA of both vertical and inclined wells [42–44]. Ma et al. [8] conducted WSA using the Mg-C criterion and a breakout width model; their results indicated that the collapse pressure of this new model is closest to the real mud weight and wellbore breakout pattern of the real field. Zhang et al. [45] evaluated the applicability of the five types of strength criteria using polyaxial strength data, and these five criteria include M-C, Drucker-Prager (D-P), ML, Mg-C, and 3D Hoek-Brown (H-B) criteria, and the stability of both vertical and inclined wells was analyzed, and they pointed out that the 3D H-B and Mg-C criteria are recommended for WSA. Maleki et al. [46] employed the M-C, H-B, and Mg-C criteria to predict the safe mud weight window (SMWW) using wireline logs, and they indicated that the Mg-C criterion is the best selection for the SMWW prediction. Chabook et al. [47] presented a collapse pressure model (CPM) for inclined wells, where the M-C, D-P, ML, and Mg-C criteria are used, and their results indicated that both ML and Mg-C criteria obtained the best results for WSA and wellbore trajectory optimization. Elyasi and Goshtasbi [48] employed M-C, H-B, and Mg-C criteria to conduct WSA, and their results indicated that the Mg-C criterion predicted the closest critical collapse pressure to the actual drilling operations. Ma et al. [49] the employed M-C and H-B criteria to conduct WSA for fractured formations, and they indicated that the H-B criterion is the best selection for WSA in fractured formations. Meng et al. [50] examined the M-C, D-P, ML, Mg-C, and 3D H-B criteria using six types of rocks, the importance of strength criteria for WSA was assessed for HP/HT drilling, and their results indicated that the ML criterion is best selection to conduct WSA. Aslannezhad et al. [51] comprehensively considered all mechanical, thermal, and chemical effects to evaluate the applicability of the six practical strength criteria in WSA, and they indicated that the ML, Mg-C, and 3D H-B criteria can predict a safer collapse pressure for shale formations, so these three criteria can be used interchangeably. Wang et al. [52] used the M-C, D-P, and Mg-C criteria to assess the wellbore collapse pressure under the five different stress regimes, and they found that various well trajectories have different selection of the best strength criteria under different stress regimes.

In the above-mentioned studies, different criteria have been developed and employed to conduct WSA, most of the studies recommended to use the M-C, Mg-C, and ML criteria for WSA [8, 38–52]. However, the collapse pressure does not comply with different strength criteria, and some of the authors indicated that the best strength criteria are different for various well trajectories under different stress regimes [52, 53]. In other words, the use of any single strength criterion is difficult to predict the collapse pressure accurately. In view of this point, Zhang et al. [53] proposed a new CPM of vertical wells by integrating the advantageous synergy among the M-C, D-P, ML, and Mg-C criteria, where each strength criterion is assigned a weight coefficient, and their results indicated that this new model can provide a much better comprehensive coverage for WSA, particularly the collapse pressure prediction. The greatest advantage of this new model is the advantageous synergy among several different criteria, but the current model is just suitable for vertical wells. Therefore, based on advantageous synergy among the M-C, Mg-C, D-P, ML, and MW-C criteria, this paper is aimed at proposing a new analytical model of WSA for inclined wells to improve the prediction accuracy of collapse pressure.

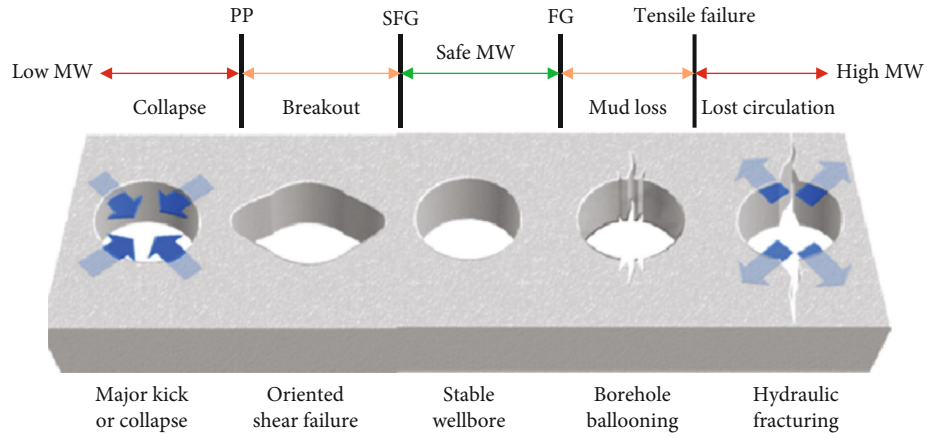


Figure 1: Relationship between mud weight and wellbore failures, modified from [19].

## 2. Stress Components on the Wall of Inclined Wellbore

To obtain the solution of stress components in the vicinity of an inclined wellbore, we made the following assumptions [19–21]: (1) the rock in the vicinity of the wellbore is homogeneous, isotropic, and linear poroelastic material; (2) the rock in the vicinity of the wellbore satisfies the hypothesis of small deformation; (3) the rock in the vicinity of the wellbore obeys the plane-strain condition; and (4) both thermal and chemical effects are ignored.

As shown in Figure 2(a), for an inclined wellbore within anisotropic horizontal stress ($\sigma_H$ and $\sigma_h$), there are three coordinates: (1) Cartesian coordinate of the in situ stresses ($x$, $y$, and $z$), where the $\sigma_v$ is parallel to the $z$-axis, the $\sigma_H$ is parallel to the $x$-axis, and the $\sigma_h$ is parallel to the $y$-axis; (2) Cartesian coordinate of the borehole ($x_b$, $y_b$, and $z_b$), where $\psi$ denotes the inclination of the borehole and $\Omega$ denotes the azimuth of the borehole relative to the $\sigma_H$ direction; and (3) cylindrical coordinate of the borehole ($r$, $\theta$, and $z_b$), where $r$ denotes the radial distance from the $z_b$-axis, $\theta$ denotes the azimuth relative to the $x_b$-axis, and $z_b$ denotes the borehole axis.

According to the solution of stress components in the vicinity of an inclined wellbore introduced by Bradley [38], on the wall of wellbore ($r = r_w$), the stress components can be written as [8, 21]

$$\begin{cases} \sigma_{rr} = (1-\delta\phi)p_m + \delta\phi p_p, \\ \sigma_{\theta\theta} = -p_m + A\sigma_h + B\sigma_H + C\sigma_v + K_1\left(p_m - p_p\right), \\ \sigma_{zz} = D\sigma_h + E\sigma_H + F\sigma_v + K_1\left(p_m - p_p\right), \\ \tau_{\theta z} = G\sigma_h + H\sigma_H + J\sigma_v, \\ \tau_{r\theta} = \tau_{rz} = 0, \end{cases} \tag{1}$$

where

$$\begin{cases} A = \cos\psi\left[\cos\psi(1-2\cos 2\theta)\sin^2\Omega + 2\sin 2\Omega \sin 2\theta\right] + (1+2\cos 2\theta)\cos^2\Omega, \\ B = \cos\psi\left[\cos\psi(1-2\cos 2\theta)\cos^2\Omega - 2\sin 2\Omega \sin 2\theta + (1+2\cos 2\theta)\sin^2\Omega\right], \\ C = (1-2\cos 2\theta)\sin^2\psi, \\ D = \sin^2\Omega\sin^2\psi + 2\nu\sin 2\Omega\cos\psi\sin 2\theta + 2\nu\cos 2\theta\left[\cos^2\Omega - \sin^2\Omega\cos^2\psi\right], \\ E = \cos^2\Omega\sin^2\psi - 2\nu\sin 2\Omega\cos\psi\sin 2\theta + 2\nu\cos 2\theta\left[\sin^2\Omega - \cos^2\Omega\cos^2\psi\right], \\ F = \cos^2\psi - 2\nu\sin^2\psi\cos 2\theta, \\ G = -\left[\sin 2\Omega\sin\psi\cos\theta + \sin^2\Omega\sin 2\psi\sin\theta\right], \\ H = \sin 2\Omega\sin\psi\cos\theta - \cos^2\Omega\sin 2\psi\sin\theta, \\ J = \sin 2\psi\sin\theta, \\ K_1 = \delta\left[\dfrac{\alpha(1-2\nu)}{1-\nu} - \phi\right], \end{cases} \tag{2}$$

where $\sigma_{rr}$, $\sigma_{\theta\theta}$, and $\sigma_{zz}$ are the radial, hoop, and axial stresses (MPa), respectively; $\tau_{\theta z}$, $\tau_{r\theta}$, and $\tau_{rz}$ are the shear stresses (MPa); $\sigma_v$, $\sigma_H$, and $\sigma_h$ are the vertical, max horizontal, and min horizontal principal stresses (MPa), respectively; $p_p$ is the pore pressure (MPa); $p_m$ is the wellbore pressure (MPa); $\Omega$ is the borehole azimuth (°); $\psi$ is the borehole inclination (°); $\theta$ is the angle of circumference relative to the $x_b$-axis (°); $\nu$ is the Poisson ratio; $\phi$ is the porosity (%); $\alpha$ is the Biot coefficient; and $\delta$ is the coefficient of seepage effect, where $\delta = 0$ denotes an impermeable wellbore, while $\delta = 1$ denotes a permeable wellbore.

As shown in Figure 2(b), the radial stress ($\sigma_{rr}$) is always one of the principal stresses, owing to it being always perpendicular to the wall of the wellbore, and the other two principal stresses must be within the plane of wellbore ($\theta, z_b$). Therefore, according to material mechanics, both normal and shear stress within the plane of wellbore ($\theta, z_b$) can be expressed as

$$\begin{cases} \sigma = \sigma_{\theta\theta}\cos^2\gamma + 2\tau_{\theta z}\cos\gamma\sin\gamma + \sigma_{zz}\sin^2\gamma, \\ \tau = \dfrac{1}{2}\left(\sigma_{zz} - \sigma_{\theta\theta}\right)\sin 2\gamma + \tau_{\theta z}\cos 2\gamma. \end{cases} \tag{3}$$

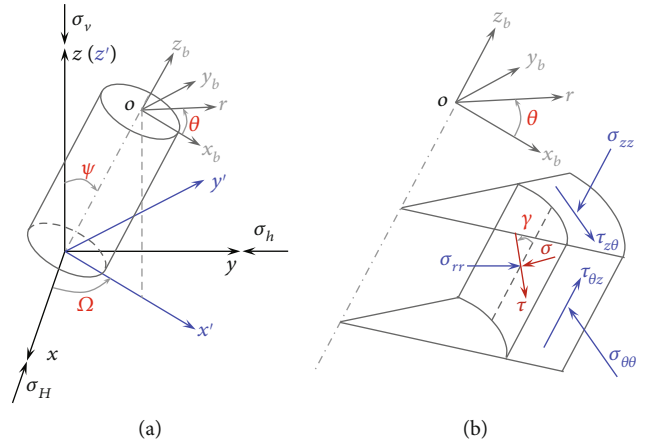


Figure 2: (a) Transformation of different coordinate systems and (b) stress components at the borehole wall.

Take the first derivative of $\sigma$ with respect to $\gamma$ to be zero, so that the direction of the major and minor principal stresses can be determined, and applying the Biot effective stress law ($\sigma' = \sigma - \alpha p_p$), the effective principal stresses (EPSs) can be written as [21]

$$\begin{cases} \sigma_1' = \sigma_1 - \alpha p_p = 0.5\left[X - 2K_1 p_p + (2K_1 - 1)p_m\right] + 0.5\sqrt{(Y - p_m)^2 + Z} - \alpha p_p, \\ \sigma_2' = \sigma_2 - \alpha p_p = 0.5\left[X - 2K_1 p_p + (2K_1 - 1)p_m\right] - 0.5\sqrt{(Y - p_m)^2 + Z} - \alpha p_p, \\ \sigma_3' = \sigma_3 - \alpha p_p = (1 - \delta\phi)p_m + \delta\phi p_p - \alpha p_p, \end{cases} \tag{4}$$

where $X$, $Y$, and $Z$ are given as

$$\begin{cases} X = (A + D)\sigma_h + (B + E)\sigma_H + (C + F)\sigma_v, \\ Y = (A - D)\sigma_h + (B - E)\sigma_H + (C - F)\sigma_v, \\ Z = 4(G\sigma_h + H\sigma_H + J\sigma_v)^2, \end{cases} \tag{5}$$

where $\sigma_1$, $\sigma_2$, and $\sigma_3$ are the major, intermediate, and minor principal stresses (MPa), respectively, and $\sigma_1'$, $\sigma_2'$, and $\sigma_3'$ are the major, intermediate, and minor EPSs (MPa), respectively.

## 3. New Collapse Pressure Model (CPM) for Inclined Wellbore

After obtaining these three EPSs on the wellbore, substituting them into different strength criteria, such as the M-C, D-P, Mg-C, ML, and MW-C criteria, the corresponding conventional CPMs can be obtained. On this basis, the real collapse pressure can be determined using the advantageous synergy among different criteria.

*3.1. CPM Based on M-C.* The M-C criterion can be written as the major and minor EPSs [26]:

$$\sigma_1' = \sigma_3' \frac{1 + \sin\varphi}{1 - \sin\varphi} + \frac{2c\cos\varphi}{1 - \sin\varphi}, \tag{6}$$

where $\varphi$ is the internal friction angle (°) and $c$ is the cohesive strength (MPa).

Substituting Equation (4) into Equation (6), the nonlinear function of collapse pressure can be written as

$$f_{\text{M-C}}(p_{m1}) = 2c\cos\varphi + \sin\varphi\left(\sigma_1' + \sigma_3'\right) - \cos\varphi(\cos 2\varphi - \sin 2\varphi) \cdot \left(\sigma_1' - \sigma_3'\right) = 0.s \tag{7}$$

The nonlinear function Equation (7) can be solved using the bisection method, and the critical wellbore pressure against wellbore collapse is the collapse pressure, i.e., $p_{c,\text{M-C}} = p_{m1}$.

*3.2. CPM Based on Mg-C.* The Mg-C criterion can be written as three EPSs [41, 42]:

$$\tau_{oct} = a + b\sigma_{m,2}, \tag{8}$$

where

$$\begin{cases} \sigma_{m,2} = \dfrac{1}{2}\left(\sigma_1' + \sigma_3'\right), \\ \tau_{\text{oct}} = \dfrac{1}{3}\left[\left(\sigma_1' - \sigma_2'\right)^2 + \left(\sigma_2' - \sigma_3'\right)^2 + \left(\sigma_3' - \sigma_1'\right)^2\right]^{1/2}, \end{cases} \tag{9}$$

$$\begin{cases} a = \dfrac{2\sqrt{2}}{3} c\cos\varphi, \\ b = \dfrac{2\sqrt{2}}{3}\sin\varphi, \end{cases} \tag{10}$$

where $\sigma_{\text{m,2}}$ is the mean normal stress (MPa), $\tau_{\text{oct}}$ is the octahedral shear stress (MPa), and $a$ and $b$ are the material constants related to $c$ and $\varphi$.

Substituting Equations (4) and (9) into Equation (8), the nonlinear function of collapse pressure can be written as

$$f_{\mathrm{Mg-C}}(p_{m3}) = a + \frac{1}{2}\left(\sigma_1' + \sigma_3'\right)b - \frac{1}{3} \cdot \left[\left(\sigma_1' - \sigma_2'\right)^2 + \left(\sigma_2' - \sigma_3'\right)^2 + \left(\sigma_3' - \sigma_1'\right)^2\right]^{1/2} = 0. \tag{11}$$

The nonlinear function Equation (11) can be solved using the bisection method, and the critical wellbore pressure against wellbore collapse is the collapse pressure, i.e., $p_{c,\mathrm{Mg-C}} = p_{m2}$.

*3.3. CPM Based on D-P.* The D-P criterion can be written as three EPSs [45]:

$$\sqrt{J_2} = k + a' I_1, \tag{12}$$

where

$$\begin{cases} I_1 = \dfrac{1}{3}\left(\sigma_1' + \sigma_2' + \sigma_3'\right), \\ J_2 = \dfrac{1}{6}\left[\left(\sigma_1' - \sigma_2'\right)^2 + \left(\sigma_2' - \sigma_3'\right)^2 + \left(\sigma_3' - \sigma_1'\right)^2\right], \end{cases} \tag{13}$$

$$\begin{cases} k = \dfrac{6c\sin\varphi}{\sqrt{3}(3 - \sin\varphi)}, \\ \alpha' = \dfrac{2\sin\varphi}{3\sqrt{3}(3 - \sin\varphi)}, \end{cases} \tag{14}$$

where $J_2$ is the second invariant of stress skew (MPa), $I_1$ is the mean effective stress (MPa), and $k$ and $a'$ are the material constants related to $c$ and $\varphi$.

Substituting Equations (4) and (13) into Equation (12), the nonlinear function of collapse pressure can be written as

$$f_{\mathrm{D-P}}(p_{m2}) = k + \frac{1}{3}a'\left(\sigma_1' + \sigma_2' + \sigma_3'\right) - \frac{1}{\sqrt{6}} \cdot \left[\left(\sigma_1' - \sigma_2'\right)^2 + \left(\sigma_2' - \sigma_3'\right)^2 + \left(\sigma_3' - \sigma_1'\right)^2\right]^{1/2} = 0. \tag{15}$$

The nonlinear function Equation (15) can be solved using bisection method, and the critical wellbore pressure against wellbore collapse is the collapse pressure, i.e., $p_{c,\mathrm{D-P}} = p_{m3}$.

*3.4. CPM Based on ML.* The ML criterion can be written as three EPSs [39, 40]:

$$\frac{I_1'^3}{I_3'} = \eta + 27, \tag{16}$$

where

$$\begin{cases} I_1' = \left(\sigma_1' + S\right) + \left(\sigma_2' + S\right) + \left(\sigma_3' + S\right), \\ I_3' = \left(\sigma_1' + S\right)\left(\sigma_2' + S\right)\left(\sigma_3' + S\right), \end{cases} \tag{17}$$

$$\begin{cases} \eta = \dfrac{4\tan^2\varphi(9 - 7\sin\varphi)}{1 - \sin\varphi}, \\ S = \dfrac{c}{\tan\varphi}, \end{cases} \tag{18}$$

where $\eta$ and $S$ are the material constants related to $c$ and $\varphi$.

Substituting Equations (4) and (17) into Equation (16), the nonlinear function of collapse pressure can be written as

$$f_{\mathrm{ML}}(p_{m4}) = \frac{\left[\left(\sigma_1' + S\right) + \left(\sigma_2' + S\right) + \left(\sigma_3' + S\right)\right]^3}{\left(\sigma_1' + S\right)\left(\sigma_2' + S\right)\left(\sigma_3' + S\right)} - \eta - 27 = 0. \tag{19}$$

The nonlinear function Equation (19) can be solved using the bisection method, and the critical wellbore pressure against wellbore collapse is the collapse pressure, i.e., $p_{c,\mathrm{ML}} = p_{m4}$.

*3.5. CPM Based on MW-C.* The MW-C criterion can be written as three EPSs [40, 51]:

$$\sqrt{J_2} = A' + B' I_1 + C' I_1^2, \tag{20}$$

where

$$\begin{cases} A' = \dfrac{\mathrm{UCS}}{\sqrt{3}} - \dfrac{\mathrm{UCS}}{3}B' - \dfrac{UCS^2}{9}C', \\ B' = \dfrac{\sqrt{3}(q-1)}{q+2} - \dfrac{C'}{3}[2\mathrm{UCS} + (q+2)\sigma_3], \\ C' = \dfrac{\sqrt{27}}{2C_1 + (q-1)\sigma_3 - \mathrm{UCS}}\left[\dfrac{C_1 + (q-1)\sigma_3 - \mathrm{UCS}}{2C_1 + (2q-1)\sigma_3 - \mathrm{UCS}} - \dfrac{q-1}{q+2}\right], \end{cases} \tag{21}$$

$$\begin{cases} \mathrm{UCS} = \dfrac{2c\cos\varphi}{1 - \sin\varphi}, \\ C_1 = (1 + 0.6\tan\varphi)\mathrm{UCS}, \\ q = \dfrac{1 + \sin\varphi}{1 - \sin\varphi}, \end{cases} \tag{22}$$

where UCS is the uniaxial compressive strength (MPa) and $A$, $B$, $C$, $q$, and $C_1$ are material constants related to $c$ and $\varphi$.

Substituting Equations (4) and (13) into Equation (20), the nonlinear function of collapse pressure can be written as

$$f_{\mathrm{MW-C}}(p_{m5}) = \frac{1}{\sqrt{6}}\left[\left(\sigma_1' - \sigma_2'\right)^2 + \left(\sigma_2' - \sigma_3'\right)^2 + \left(\sigma_3' - \sigma_1'\right)^2\right]^{1/2} - A' - \frac{1}{3}B'\left(\sigma_1' + \sigma_2' + \sigma_3'\right) - \frac{1}{9}C'\left(\sigma_1' + \sigma_2' + \sigma_3'\right)^2 = 0. \tag{23}$$

The nonlinear function Equation (23) can be solved using the bisection method, and the critical wellbore pressure against wellbore collapse is the collapse pressure, i.e., $p_{c,\mathrm{MW-C}} = p_{m5}$.

*3.6. New CPM Based on the Advantageous Synergy among Different Criteria.* Different criteria have been developed or employed to conduct WSA, but the collapse pressure does not comply with different strength criteria, and some of the authors indicated that the best strength criteria are different for various well trajectories under different stress regimes [52, 53]. Zhang et al. [53] integrated the advantageous synergy among the M-C, D-P, ML, and Mg-C criteria to propose a new CPM of vertical wells, the advantageous synergy among different strength criteria assumes that each strength criterion has a different weight coefficient, and the real collapse pressure should be determined by combining both conventional CPMs and their corresponding weight coefficient. However, this method can just be suitable for vertical wells. To extend the applicable conditions of this advantageous synergy effect of different criteria, we employed the similar principle to develop a new CPM based on the advantageous synergy among the five different strength criteria, and this new CPM can be written as

$$p_c = \omega_1 p_{m1} + \omega_2 p_{m2} + \omega_3 p_{m3} + \omega_4 p_{m4} + \omega_5 p_{m5}, \tag{24}$$

where $p_{m1}$, $p_{m2}$, $p_{m3}$, $p_{m4}$, and $p_{m5}$ are the critical collapse pressure corresponding to the M-C, Mg-C, D-P, ML, and MW-C criteria (MPa), respectively; $p_c$ is the critical collapse pressure of this new CPM (MPa); and $\omega_1$, $\omega_2$, $\omega_3$, $\omega_4$, and $\omega_5$ are the weight coefficients related to the M-C, Mg-C, D-P, ML, and MW-C criteria, respectively.

Due to the introduction of weight coefficients, this new analytical model of collapse pressure of inclined wellbore can involve the advantageous synergy effect of different criteria. According to Equation (32), this new analytical model can be simplified as the conventional analytical model by adjusting the weight coefficients: (1) when $\omega_1 = 1$ and $\omega_2 = \omega_3 = \omega_4 = \omega_5 = 0$, this new CPM can be simplified as the conventional analytical CPM based on M-C criterion. (2) When $\omega_2 = 1$ and $\omega_1 = \omega_3 = \omega_4 = \omega_5 = 0$, this new CPM can be simplified as the conventional analytical CPM based on Mg-C criterion. (3) When $\omega_3 = 1$ and $\omega_1 = \omega_2 = \omega_4 = \omega_5 = 0$, this new CPM can be simplified as the conventional analytical CPM based on D-P criterion. (4) When $\omega_4 = 1$ and $\omega_1 = \omega_2 = \omega_3 = \omega_5 = 0$, this new CPM can be simplified as the conventional analytical CPM based on ML criterion. (5) When $\omega_5 = 1$ and $\omega_1 = \omega_2 = \omega_3 = \omega_4 = 0$, this new CPM can be simplified as the conventional analytical CPM based on MW-C criterion.

On this basis, the weight coefficients can be determined by comparing the relative importance of different strength criteria, and the following procedure can be utilized to determine the weight coefficients using analytic hierarchy process (AHP) [53, 54]:

(1) Conduct $N$ groups of rock mechanics tests of rock samples collected from the drilled formation under different confining pressures. Then, the M-C, D-P, Mg-C, ML, and MW-C criteria are employed to calculate the strength of triaxial compression, and the testing results are fitted with the calculating results

(2) The number of rock samples that obey the M-C criterion is counted as $n_1$; similarly, the number of rock samples that obey the Mg-C, D-P, ML, and MW-C criteria is counted as $n_2$, $n_3$, $n_4$, and $n_5$, $n_2 + n_2 + n_3 + n_4 + n_5 = N$. The standard of determination agreement between testing and calculating results is the relative error < 3%

(3) Calculate the ratio $(n_i/n_j)$ of any given two numbers of rock samples that obey different criteria to obtain the relative importance $(a_{ij})$ of any given two strength criteria $i$ and $j$, where the relative importance $(a_{ij})$ means the relative importance of strength criterion $i$ to $j$; its value is determined by the expert according to the ratio $(n_i/n_j)$ and the ratio-scaled table (as shown in Table 1). In general, $a_{ij} = 1/a_{ji}$, $a_{ii} = 1$, and $a_{ij} > 0$

(4) Establish the discriminant matrix $\mathbf{\Lambda}$ between different strength criteria using Equation (25); then, calculate the eigenvector of the discriminant matrix $\mathbf{\Lambda}$ using Equation (26).

$$\Lambda = \begin{bmatrix} \mathrm{M-C} & a_{11} & a_{12} & a_{13} & a_{14} & a_{15} \\ \mathrm{Mg-C} & a_{21} & a_{22} & a_{23} & a_{24} & a_{25} \\ \mathrm{D-P} & a_{31} & a_{32} & a_{33} & a_{34} & a_{35} \\ \mathrm{ML} & a_{41} & a_{42} & a_{43} & a_{44} & a_{45} \\ \mathrm{MW-C} & a_{51} & a_{52} & a_{53} & a_{54} & a_{55} \\ & \mathrm{M-C} & \mathrm{Mg-C} & \mathrm{D-P} & \mathrm{ML} & \mathrm{MW-C} \end{bmatrix}, \tag{25}$$

$$W = (\omega_1, \omega_2, \omega_3, \omega_4, \omega_5)^T = \left(\frac{\bar{W}_1}{\sum_{i=1}^5 \bar{W}_i}, \frac{\bar{W}_2}{\sum_{i=1}^5 \bar{W}_i}, \frac{\bar{W}_3}{\sum_{i=1}^5 \bar{W}_i}, \frac{\bar{W}_4}{\sum_{i=1}^5 \bar{W}_i}, \frac{\bar{W}_5}{\sum_{i=1}^5 \bar{W}_i}\right)^T, \tag{26}$$

Table 1: Ratio-scaled table.

| Criterion $i$ to $j$ | $a_{ij}$ |
|---|---|
| Equally important | 1 |
| A little important | 3 |
| Comparatively important | 5 |
| Strongly important | 7 |
| Extremely important | 9 |
| Intermediate value of two adjacent judgments | 2, 4, 6, 8 |

where

$$\bar{W}_i = \frac{a_{11}}{\sum_{i=1}^{5} a_{i1}} + \frac{a_{12}}{\sum_{i=1}^{5} a_{i2}} + \frac{a_{13}}{\sum_{i=1}^{5} a_{i3}} + \frac{a_{14}}{\sum_{i=1}^{5} a_{i4}} + \frac{a_{15}}{\sum_{i=1}^{5} a_{i5}} \tag{27}$$

(5) Conduct the consistency testing of weight coefficient to determine its validity, and the consistency ratio (CR) expressed by Equation (28) is usually used. When CR < 0.1, it satisfies the requirement of consistency test; then, the normalized feature vector $\boldsymbol{W}$ can be the weight coefficients. However, if the CR does not satisfy the requirement of consistency test, the discriminant matrix $\boldsymbol{\Lambda}$ should be reconstructed [53, 54].

$$\mathrm{CR} = \frac{\mathrm{CI}}{\mathrm{RI}}, \tag{28}$$

where

$$\mathrm{CI} = \frac{\lambda_{\max} - n}{n-1} = \frac{\lambda_{\max} - 5}{4}, \tag{29}$$

$$\lambda_{\max} = \frac{1}{n}\sum_{i=1}^{n} \frac{(\boldsymbol{\Lambda W})_i}{\omega_i} = \frac{1}{5}\sum_{i=1}^{5} \frac{(\boldsymbol{\Lambda W})_i}{\omega_i}, \tag{30}$$

where CR is the consistency ratio; RI is the random consistency index, RI = 1.12; CI is the consistency index; $\lambda_{\max}$ is the characteristic value of the discriminant matrix $\boldsymbol{\Lambda}$; $(\boldsymbol{\Lambda W})_i$ is the $i^{\text{th}}$ component of $\boldsymbol{\Lambda W}$; and $n$ is the number of strength criteria.

On this basis, the use of CPM described in Equation (24) needs to determine the weight coefficients corresponding to the M-C, Mg-C, D-P, ML, and MW-C criteria, and according to the AHP method mentioned above, the discriminant matrix $\boldsymbol{\Lambda}$ between different strength criteria can be expressed as

$$\Lambda = \begin{bmatrix} \mathrm{M-C} & 1 & \frac{1}{4} & 6 & 5 & 2 \\ \mathrm{Mg-C} & 4 & 1 & 7 & 6 & 4 \\ \mathrm{D-P} & \frac{1}{6} & \frac{1}{7} & 1 & \frac{1}{2} & \frac{1}{7} \\ \mathrm{ML} & \frac{1}{5} & \frac{1}{6} & 2 & 1 & \frac{1}{6} \\ \mathrm{MW-C} & \frac{1}{2} & \frac{1}{4} & 7 & 6 & 1 \\ & \mathrm{M-C} & \mathrm{Mg-C} & \mathrm{D-P} & \mathrm{ML} & \mathrm{MW-C} \end{bmatrix}. \tag{31}$$

Then, normalize each column of the discriminant matrix $\boldsymbol{\Lambda}$, and sum up the rows to get the column vectors, and the eigenvectors can be obtained by normalization of this column vector:

$$W = (\omega_1, \omega_2, \omega_3, \omega_4, \omega_5)^T = (0.22, 0.48, 0.04, 0.06, 0.20)^T. \tag{32}$$

Equation (32) is the column vector of weight coefficients; to determine its validity, the consistency test of weight coefficient should be conducted. According to Equations (28)–(30), the CR can be determined as follows:

$$\begin{aligned} \mathrm{CR} &= \frac{\mathrm{CI}}{\mathrm{RI}} \\ &= \frac{\left(1/5\sum_{i=1}^{5}\left((\Lambda W)_i/\omega_i\right) - 5\right)/4}{1.12} \\ &= \frac{(5.4-5)/4}{1.12} \\ &= \frac{0.1}{1.12} \\ &= 0.089, \end{aligned} \tag{33}$$

Owing CR = 0.089 < 0.1, so as to it satisfies the requirement of consistency test. Thus, the weight coefficients are equal to the components of the normalized feature vector $\boldsymbol{W}$. Therefore, this new CPM can be expressed as

$$p_c = 0.22p_{m1} + 0.48p_{m2} + 0.04p_{m3} + 0.06p_{m4} + 0.20p_{m5}. \tag{34}$$

## 4. WSA Results of Inclined Wellbore under Different Stress Regimes

To compare the analysis results of wellbore stability among this new analytical model and the conventional analytical models, the basic parameters collected from Sichuan Basin of China were used, where the in situ stresses are rounded and listed in Table 2, and the other parameters are as follows: the true vertical depth (TVD) of 3100 m, the porosity of 10%, the Poisson ratio of 0.25, the coefficient of seepage effect of 0, the Biot coefficient of 0.8, the cohesive strength of 21 MPa, and the internal friction angle of 32°. In

Table 2: Basic parameters of in situ stress.

| Case | Stress regimes | $\sigma_v$ (MPa/100 m) | $\sigma_H$ (MPa/100 m) | $\sigma_h$ (MPa/100 m) | $p_p$ (g/cm$^3$) | Azimuth of $\sigma_H$ (°) |
|---|---|---|---|---|---|---|
| 1 | NF ($\sigma_v > \sigma_H > \sigma_h$) | 3.0581 | 2.7183 | 2.3785 | 1.1893 | N30°E |
| 2 | SSF ($\sigma_H > \sigma_v > \sigma_h$) | 2.5484 | 2.7183 | 2.3785 | 1.1893 | N30°E |
| 3 | RF ($\sigma_H > \sigma_h > \sigma_v$) | 2.2086 | 2.7183 | 2.3785 | 1.1893 | N30°E |

Table 2, three kinds of the most commonly encountered stress regimes, such as the normal fault (NF), strike-slip fault (SSF), and reverse fault (RF), are involved to reveal the difference of different stress regimes.

To present the calculated results of CPM, it has been converted as equivalent mud weight (EMW) by using the collapse pressure divided by $0.00981 \times \mathrm{TVD}$. The lower hemisphere projection plot is employed to present the wellbore collapse pressure versus well path (inclination and azimuth angle) in a much better way, and its principle is shown in Figure 3, where the concentric circle denotes the borehole inclination, while the radial line denotes the borehole azimuth.

*4.1. WSA Results under NF Condition.* Under the NF condition, the stability analysis results of the inclined wellbore using different strength criteria are shown in Figure 4. The following are clearly found:

(1) As shown in Figure 4(a), for M-C criterion, the EMW of collapse pressure increased with borehole inclination along the $\sigma_H$ direction, while it decreased and then increased with borehole inclination along the $\sigma_h$ direction. The EMW of collapse pressure was between 1.16 g/cm$^3$ and 1.45 g/cm$^3$, the inclined well ($\psi \approx 42\circ$) along the $\sigma_h$ direction had the best stability, the horizontal well along the $\sigma_H$ direction had the worst stability, and the stability of horizontal and highly deviated wells parallel to the $\sigma_h$ direction was better than that of $\sigma_H$ direction

(2) As shown in Figure 4(b), for Mg-C criterion, the EMW of collapse pressure increased with borehole inclination along the $\sigma_H$ direction, while it decreased and then increased with borehole inclination along the $\sigma_h$ direction. The EMW of collapse pressure was between 0.93 g/cm$^3$ and 1.17 g/cm$^3$, and the inclined well ($\psi \approx 42\circ$) along the $\sigma_h$ direction had the best stability, while the horizontal well along the $\sigma_H$ direction had the worst stability, and the stability of horizontal and highly deviated wells parallel to the $\sigma_h$ direction was slightly better than the $\sigma_H$ direction

(3) As shown in Figure 4(c), for D-P criterion, the EMW of collapse pressure always increased with borehole inclination along either the $\sigma_H$ direction or the $\sigma_h$ direction. The EMW of collapse pressure ranged from 0.82 g/cm$^3$ to 1.17 g/cm$^3$, and the vertical well had the best stability, while the horizontal well along the $\sigma_h$ direction had the worst stability, and the stability of horizontal and highly deviated wells parallel to the $\sigma_H$ direction was better than the $\sigma_h$ direction, and this phenomenon was surely different with the others, because of the different influence of the $\sigma_2$ for different criteria

(4) As shown in Figure 4(d), for ML criterion, the EMW of collapse pressure increased with borehole inclination along the $\sigma_H$ direction, while it decreased and then increased with borehole inclination along the $\sigma_h$ direction. The EMW of collapse pressure was between 0.88 g/cm$^3$ and 1.11 g/cm$^3$, and the inclined well ($\psi \approx 42\circ$) along the $\sigma_h$ direction had the best stability, while the horizontal well along the $\sigma_H$ direction had the worst stability, and the stability of horizontal and highly deviated wells parallel to the $\sigma_h$ direction was slightly better than that of $\sigma_H$ direction

(5) As shown in Figure 4(e), for MW-C criterion, the EMW of collapse pressure increased with borehole inclination along the $\sigma_H$ direction, while it decreased and then increased with borehole inclination along the $\sigma_h$ direction. The EMW of collapse pressure was between 0.84 g/cm$^3$ and 1.12 g/cm$^3$, and the inclined well ($\psi \approx 42\circ$) along the $\sigma_h$ direction had the best stability, while the horizontal well along the $\sigma_H$ direction had the worst stability, and the stability of horizontal and highly deviated wells parallel to the $\sigma_h$ direction was slightly better than that of $\sigma_H$ direction

(6) As shown in Figure 4(f), for this new CPM, the EMW of collapse pressure increased with borehole inclination along the $\sigma_H$ direction, while it firstly decreased and then increased with borehole inclination along the minimum horizontal stress. The EMW of collapse pressure was between 0.96 g/cm$^3$ and 1.22 g/cm$^3$, and the inclined well ($\psi \approx 42\circ$) along the $\sigma_h$ direction had the best stability, while the horizontal well along the $\sigma_H$ direction had the worst stability, and the stability of horizontal and highly deviated wells parallel to the $\sigma_h$ direction was slightly better than that of $\sigma_H$ direction

(7) For the same well path condition, as shown in Figure 4, the M-C criterion always gave the greatest collapse pressure owing to it ignoring the influence of the $\sigma_2$, followed by this new CPM, the Mg-C criterion, the MW-C criterion, the ML criterion, and the D-P criterion, because the other conventional models involved the different influence of the $\sigma_2$

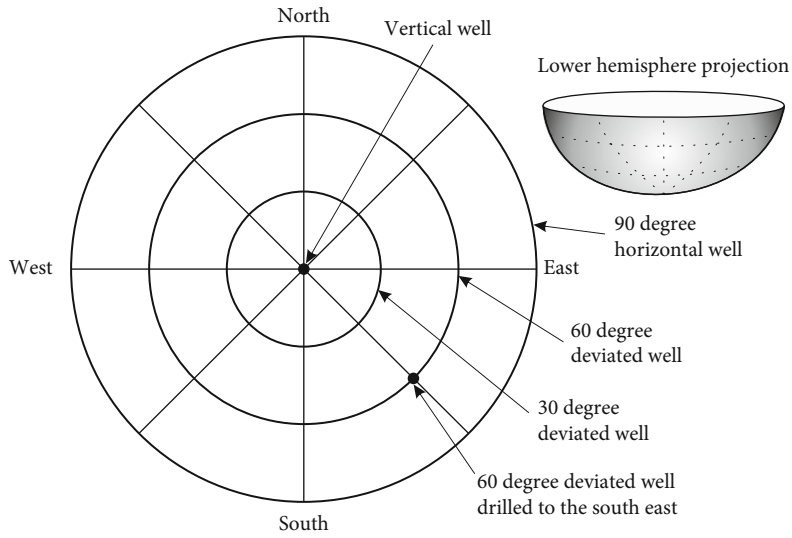


Figure 3: Schematic plot of the lower hemisphere projection [8].

[55, 56], and this new CPM integrated the advantageous synergy of the five different criteria

*4.2. WSA Results under SSF Condition.* Under the SSF condition, the stability analysis results of the inclined wellbore using different strength criteria are shown in Figure 5. The following are clearly found:

(1) As shown in Figure 5(a), for M-C criterion, the EMW of collapse pressure decreased with borehole inclination either along either the $\sigma_H$ direction or the $\sigma_h$ direction. The EMW of collapse pressure was between 1.07 g/cm$^3$ and 1.22 g/cm$^3$, and the horizontal well deviated ~45° from the $\sigma_H$ direction had the best stability, while the vertical well had the worst stability, and the stability of horizontal and highly deviated wells parallel to the $\sigma_H$ direction was surely better than that of $\sigma_h$ direction

(2) As shown in Figure 5(b), for Mg-C criterion, the EMW of collapse pressure decreased with borehole inclination either along either the $\sigma_H$ direction or the $\sigma_h$ direction. The EMW of collapse pressure was between 0.85 g/cm$^3$ and 0.97 g/cm$^3$, and the horizontal well deviated ~45° from the $\sigma_H$ direction had the best stability, while the vertical well had the worst stability, and the stability of horizontal and highly deviated wells parallel to the $\sigma_H$ direction was surely better than that of $\sigma_h$ direction

(3) As shown in Figure 5(c), for D-P criterion, the EMW of collapse pressure increased with borehole inclination along the $\sigma_h$ direction, while it decreased with borehole inclination along the $\sigma_H$ direction. The EMW of collapse pressure was between 0.79 g/cm$^3$ and 0.96 g/cm$^3$, and the horizontal well along the $\sigma_H$ direction had the best stability, while the horizontal well along the $\sigma_h$ direction had the worst stability, and the stability of horizontal and highly deviated wells parallel to the $\sigma_H$ direction was surely better than that of $\sigma_h$ direction

(4) As shown in Figure 5(d), for ML criterion, the EMW of collapse pressure decreased with borehole inclination along either the $\sigma_H$ direction or the $\sigma_h$ direction. The EMW of collapse pressure was between 0.81 g/cm$^3$ and 0.93 g/cm$^3$, and the horizontal well deviated ~45° from the $\sigma_H$ direction had the best stability, while the vertical well had the worst stability, and the stability of horizontal and highly deviated wells parallel to the $\sigma_H$ direction was slightly better than that of $\sigma_h$ direction

(5) As shown in Figure 5(e), for MW-C criterion, the EMW of collapse pressure decreased with borehole inclination along either the $\sigma_H$ direction or the $\sigma_h$ direction. The EMW of collapse pressure was between 0.75 g/cm$^3$ and 0.89 g/cm$^3$, and the horizontal well deviated ~45° from the $\sigma_H$ direction had the best stability, while the vertical well had the worst stability, and the stability of horizontal and highly deviated wells parallel to the $\sigma_H$ direction was slightly better than the $\sigma_h$ direction

(6) As shown in Figure 5(f), for this new CPM, the EMW of collapse pressure decreased with borehole inclination along either the $\sigma_H$ direction or the $\sigma_h$ direction. The EMW of collapse pressure was between 0.87 g/cm$^3$ and 1.01 g/cm$^3$, and the horizontal well deviated ~45° from the $\sigma_H$ direction had the best stability, while the vertical well had the worst stability, and the stability of horizontal and highly deviated wells parallel to the $\sigma_H$ direction was surely better than that of $\sigma_h$ direction

(7) For the same well path condition, as shown in Figure 5, the M-C criterion always gave the greatest collapse pressure owing to it ignoring the influence

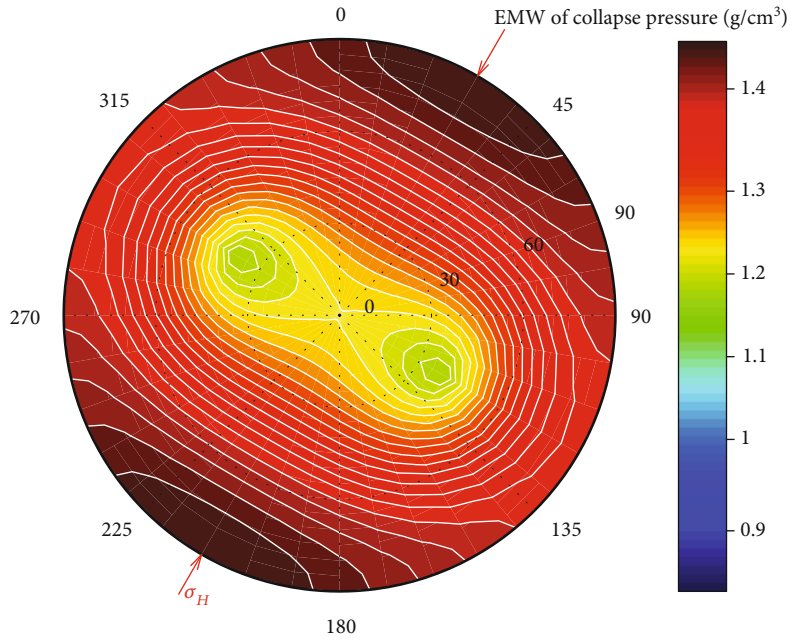


(a) M-C

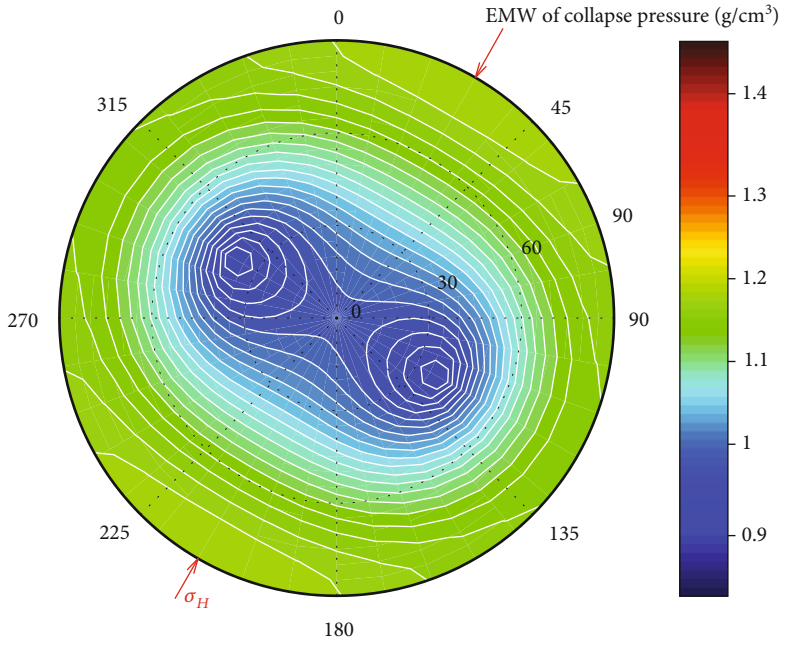


(b) Mg-C

Figure 4: Continued.

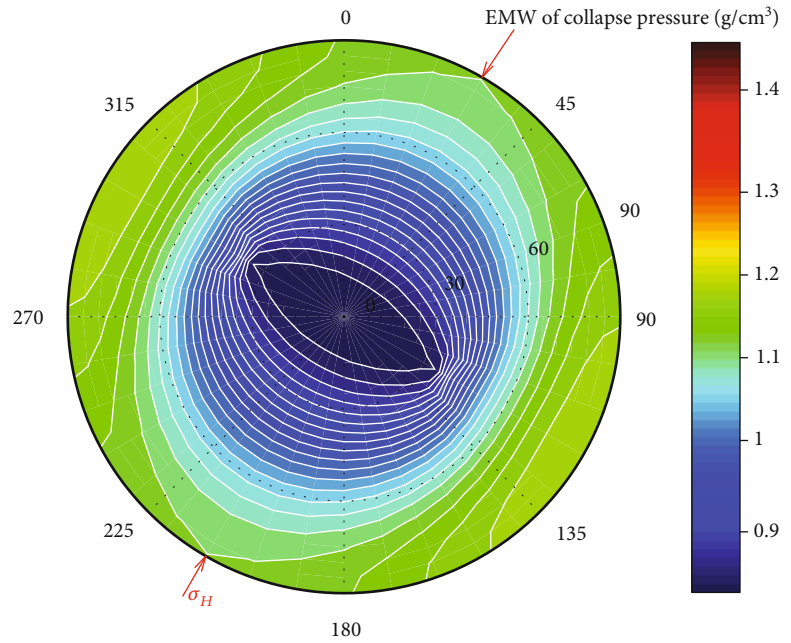


(c) D-P

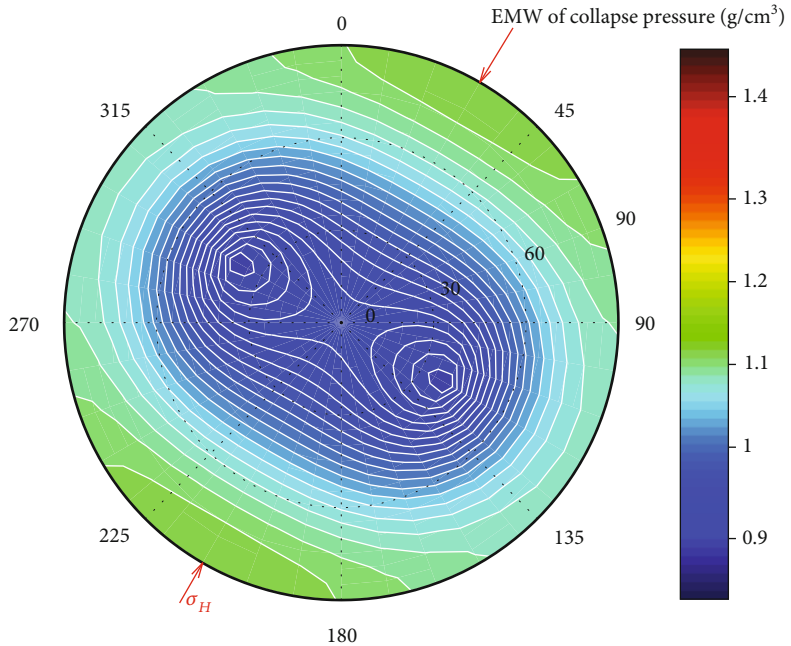


(d) ML

Figure 4: Continued.

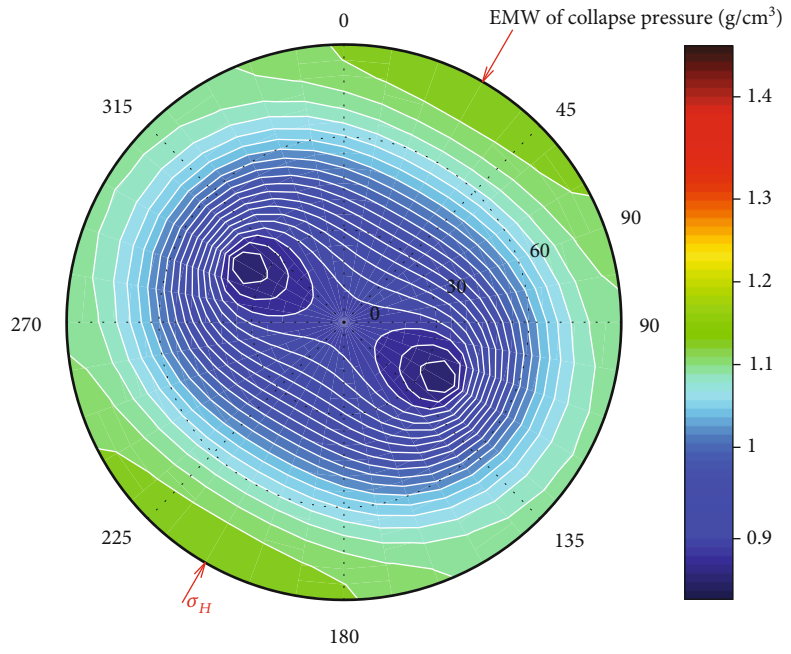


(e) MW-C

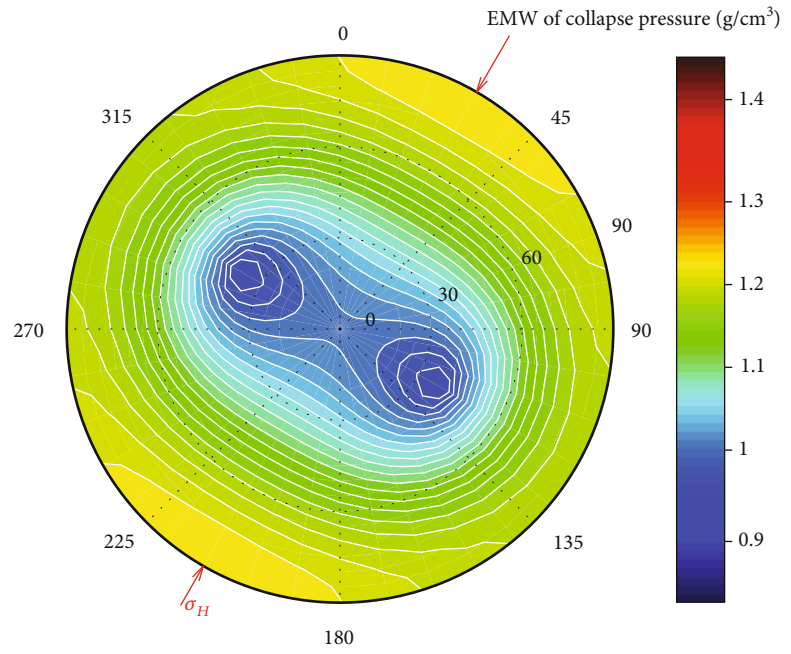


(f) New model

Figure 4: Lower hemisphere projection plot of collapse pressure for inclined wellbore under NF.

of the $\sigma_2$, followed by this new CPM, the Mg-C criterion, the D-P criterion, the ML criterion, and the MW-C criterion, because the other conventional models involved the different influence of the $\sigma_2$ [55, 56], and this new CPM integrated the advantageous synergy of the five different criteria

*4.3. WSA Results under RF Condition.* Under the RF condition, the stability analysis results of the inclined wellbore are shown in Figure 6. The following are clearly found:

(1) As shown in Figure 6(a), for M-C criterion, the EMW of collapse pressure increased with borehole inclination along the $\sigma_h$ direction, while it decreased and then increased slightly with borehole inclination along the $\sigma_H$ direction. The EMW of collapse pressure was between 0.99 g/cm$^3$ and 1.26 g/cm$^3$, and the inclined well ($\psi \approx 60^\circ$) along the $\sigma_H$ direction had the best stability, while the horizontal well along the $\sigma_h$ direction had the worst stability, and the stability of horizontal and highly deviated wells parallel

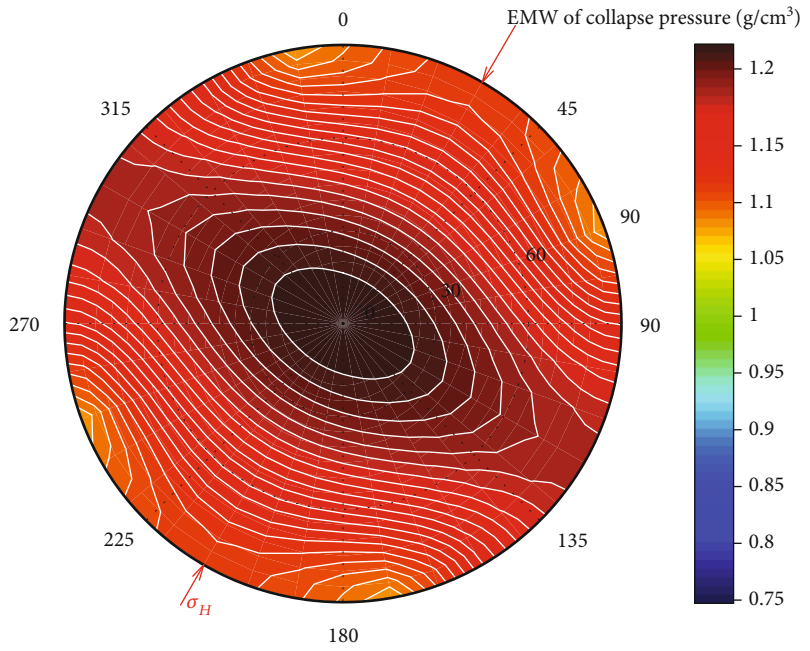


(a) M-C

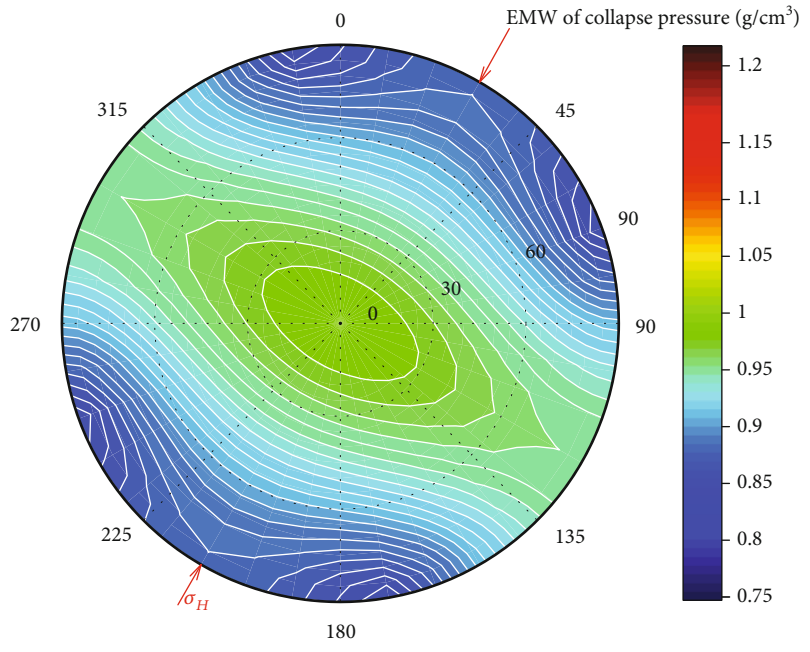


(b) Mg-C

Figure 5: Continued.

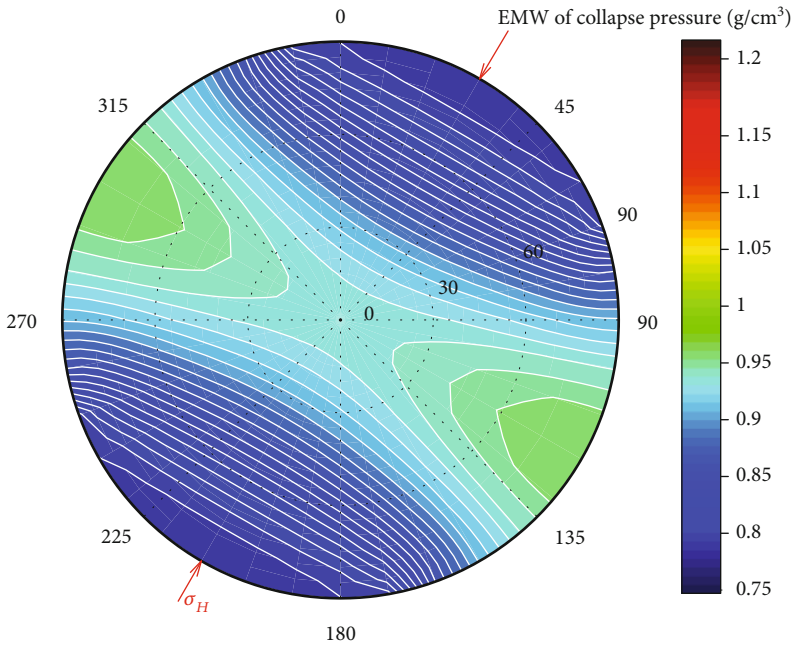


(c) D-P

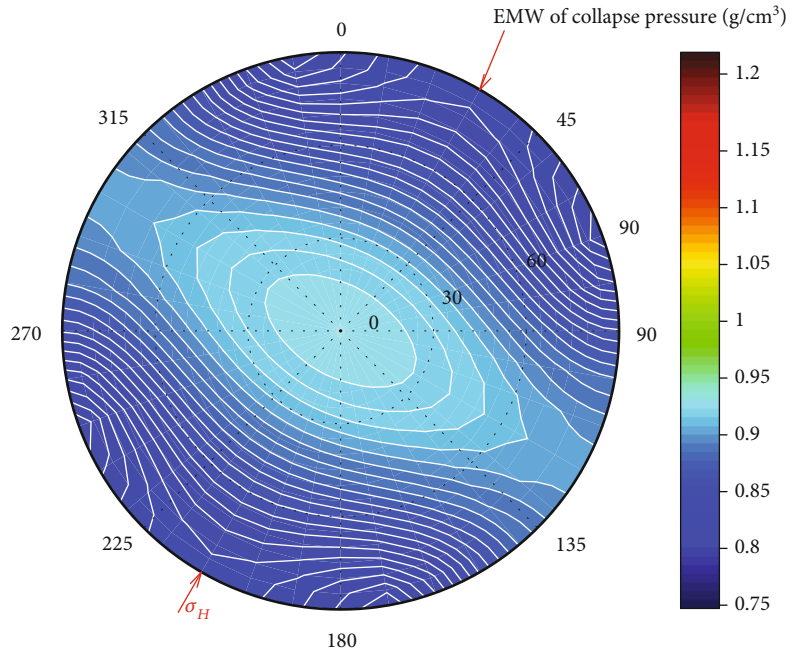


(d) ML

Figure 5: Continued.

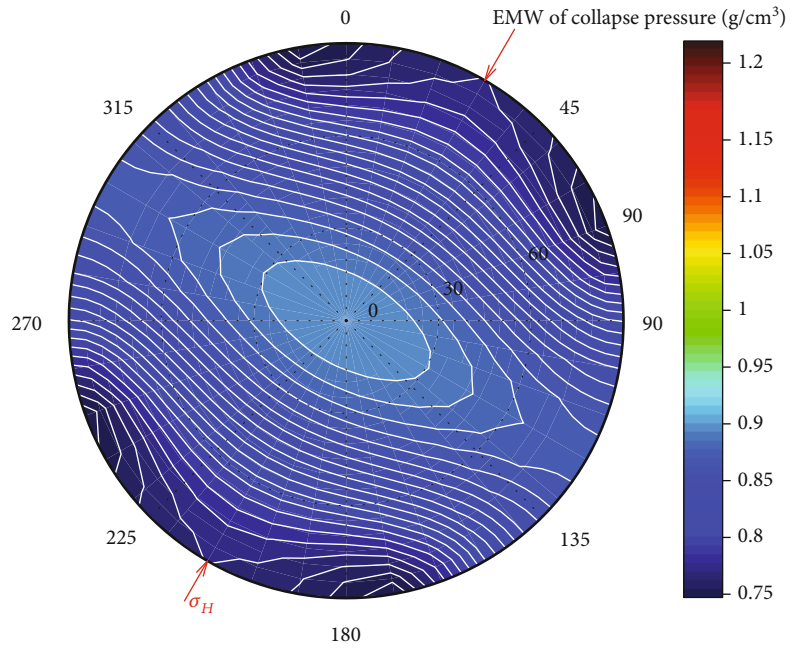


(e) MW-C

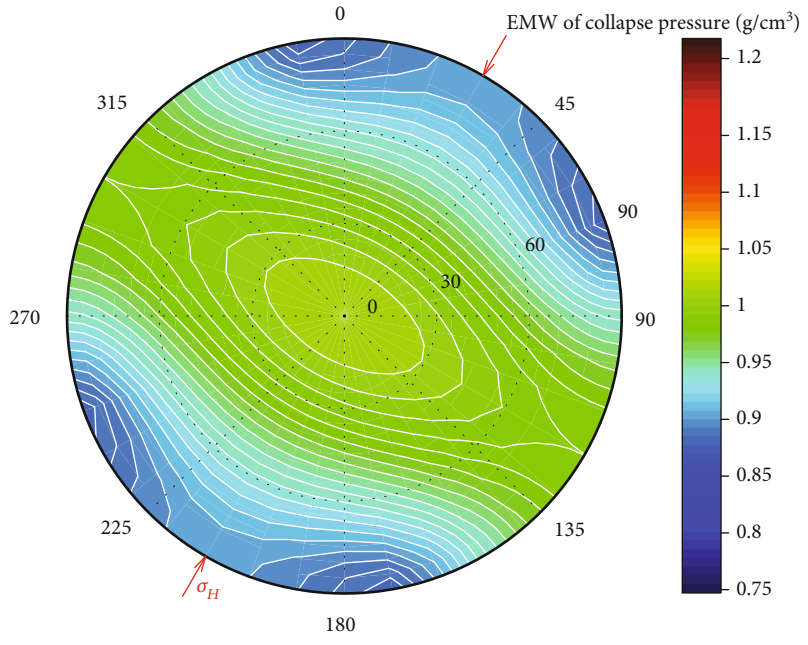


(f) New model

Figure 5: Lower hemisphere projection plot of collapse pressure for inclined wellbore under SSF.

to the $\sigma_H$ direction was surely better than that of $\sigma_h$ direction

(2) As shown in Figure 6(b), for Mg-C criterion, the EMW of collapse pressure slightly increased with borehole inclination along the $\sigma_h$ direction, while it decreased and then increased slightly with borehole inclination along the $\sigma_H$ direction. The EMW of collapse pressure was between 0.78 g/cm$^3$ and 1.01 g/cm$^3$, and the inclined well ($\psi \approx 60\circ$) along the $\sigma_H$ direction had the best stability, while the horizontal well along the $\sigma_h$ direction had the worst stability, and the stability of horizontal and highly deviated wells parallel to the $\sigma_H$ direction was surely better than that of $\sigma_h$ direction

(3) As shown in Figure 6(c), for D-P criterion, the EMW of collapse pressure decreased with borehole inclination along either the $\sigma_H$ direction or the $\sigma_h$ direction. The EMW of collapse pressure was between 0.71 g/cm$^3$

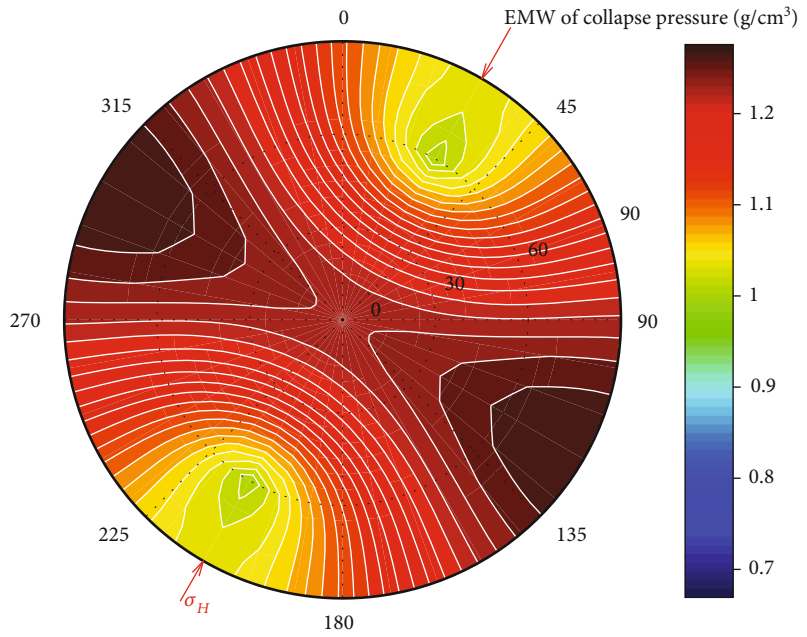


(a) M-C

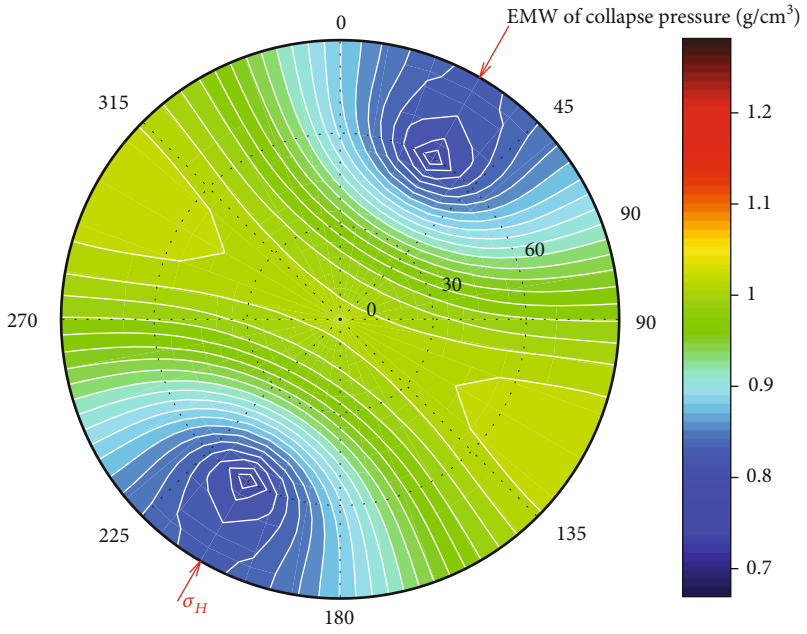


(b) Mg-C

Figure 6: Continued.

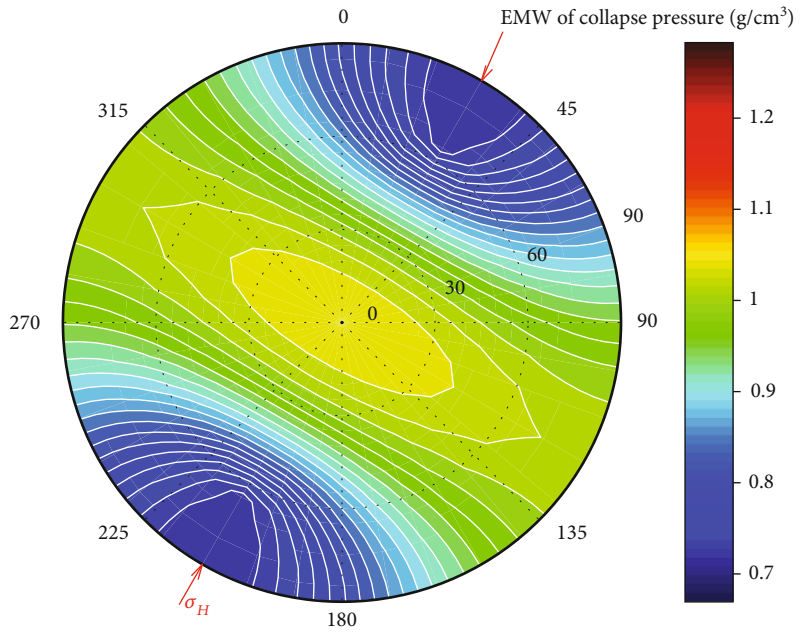


(c) D-P

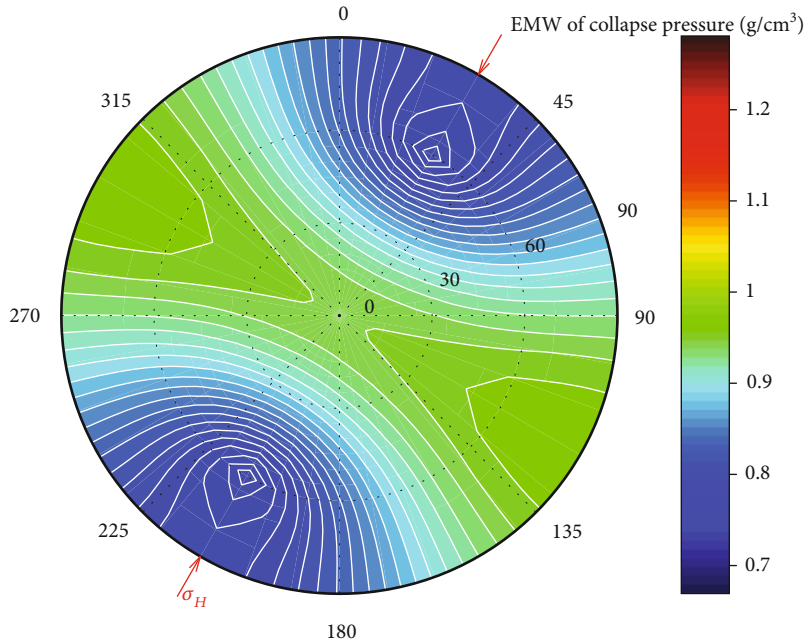


(d) ML

Figure 6: Continued.

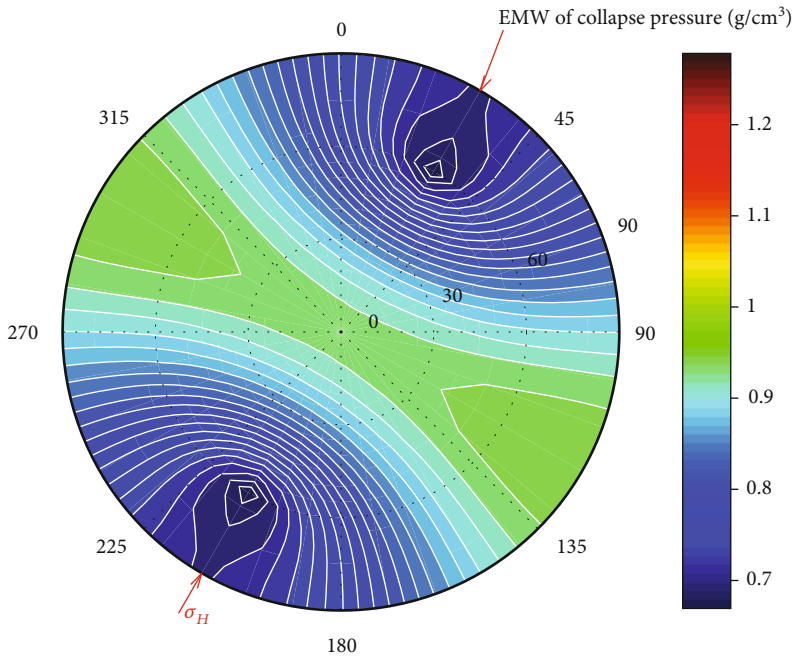


(e) MW-C

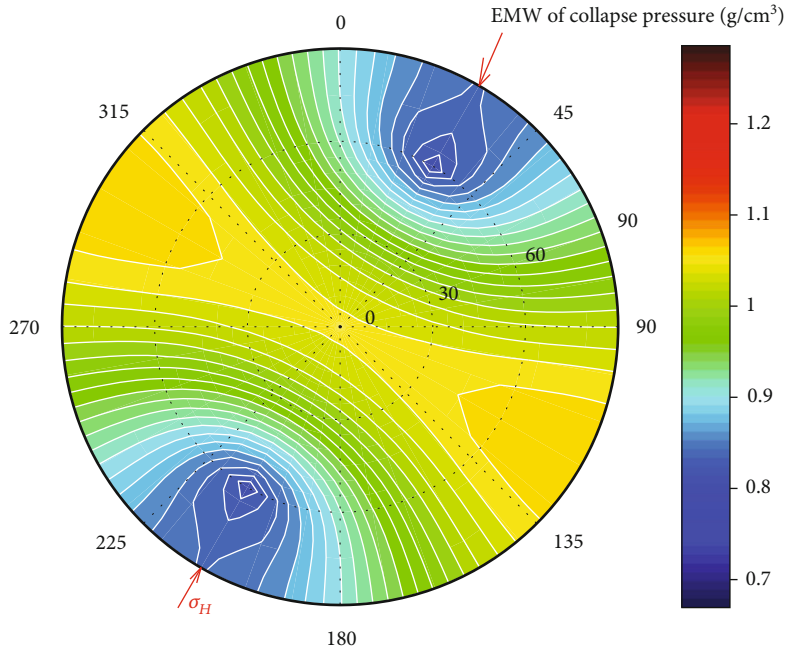


(f) New model

Figure 6: Lower hemisphere projection plot of collapse pressure for inclined wellbore under RF.

and 1.03 g/cm$^3$, and the highly deviated and horizontal wells ($\psi \approx 62 - 90\circ$) along the $\sigma_H$ direction had the best stability, while the vertical well had the worst stability, and the stability of horizontal and highly deviated wells parallel to the $\sigma_H$ direction was surely better than that of $\sigma_h$ direction

(4) As shown in Figure 6(d), for ML criterion, the EMW of collapse pressure slightly increased with borehole inclination along the $\sigma_h$ direction, while it decreased and then increased slightly with borehole inclination along the $\sigma_H$ direction. The EMW of collapse pressure was between 0.74 g/cm$^3$ and 0.96 g/cm$^3$, and the inclined well ($\psi \approx 60\circ$) along the $\sigma_H$ direction had the best stability, while the horizontal well along the $\sigma_h$ direction had the worst stability, and the stability of horizontal and highly deviated wells parallel to the $\sigma_H$ direction was surely better than that of $\sigma_h$ direction

Table 3: EMW ranges of collapse pressure with different models under different stress regimes.

| Case | Stress regimes | Variation range of EMW of collapse pressure (g/cm$^3$) | | | | | |
|---|---|---|---|---|---|---|---|
| | | M-C | Mg-C | D-P | ML | MW-C | New model |
| 1 | NF | 1.16-1.45 | 0.93-1.17 | 0.82-1.17 | 0.88-1.11 | 0.84-1.12 | 0.96-1.22 |
| 2 | SSF | 1.07-1.22 | 0.85-0.97 | 0.79-0.96 | 0.81-0.93 | 0.75-0.89 | 0.87-1.01 |
| 3 | RF | 0.99-1.26 | 0.78-1.01 | 0.71-1.03 | 0.74-0.96 | 0.67-0.94 | 0.80-1.05 |

Table 4: Best/worst well paths for wellbore stability under different stress regimes.

| Case | Stress regimes | Most/worst stable well path | | | | | |
|---|---|---|---|---|---|---|---|
| | | M-C | Mg-C | D-P | ML | MW-C | This new CPM |
| 1 | NF | Inclined/horizontal | Inclined/horizontal | Vertical/horizontal | Inclined/horizontal | Inclined/horizontal | Inclined/horizontal |
| 2 | SSF | Horizontal/vertical | Horizontal/vertical | Horizontal/horizontal | Horizontal/vertical | Horizontal/vertical | Horizontal/vertical |
| 3 | RF | Inclined/horizontal | Inclined/horizontal | Inclined/vertical | Inclined/horizontal | Inclined/horizontal | Inclined/horizontal |

(5) As shown in Figure 6(e), for MW-C criterion, the EMW of collapse pressure slightly increased with borehole inclination along the $\sigma_h$ direction, while it firstly decreased and then increased slightly with borehole inclination along the $\sigma_H$ direction. The EMW of collapse pressure was between 0.67 g/cm$^3$ and 0.94 g/cm$^3$, and the inclined well ($\psi \approx 60^\circ$) along the $\sigma_H$ direction had the best stability, while the horizontal well along the $\sigma_h$ direction had the worst stability, and the stability of horizontal and highly deviated wells parallel to the $\sigma_H$ direction was surely better than that of $\sigma_h$ direction

(6) As shown in Figure 6(f), for this new CPM, the EMW of collapse pressure slightly increased with borehole inclination along the $\sigma_h$ direction, while it firstly decreased and then increased slightly with borehole inclination along the $\sigma_H$ direction. The EMW of collapse pressure was between 0.80 g/cm$^3$ and 1.05 g/cm$^3$, and the inclined well ($\psi \approx 60^\circ$) along the $\sigma_H$ direction had the best stability, while the horizontal well along the $\sigma_h$ direction had the worst stability, and the stability of horizontal and highly deviated wells parallel to the $\sigma_H$ direction was surely better than that of $\sigma_h$ direction

(7) For the same well path condition, as shown in Figure 6, the M-C criterion always gave the greatest collapse pressure owing to it ignoring the influence of the $\sigma_2$, followed by this new CPM, the Mg-C criterion, the ML criterion, the D-P criterion, and the MW-C criterion, because the other conventional models involved the different influence of the $\sigma_2$ [55, 56], and this new CPM integrated the advantageous synergy of the five different criteria

*4.4. Comparison of Different Stress Regimes.* Table 3 lists the EMW ranges of collapse pressure of different models under different stress regimes. As shown in Figure 4 and Table 3, for the same well path under the NF condition, the M-C criterion always gave the greatest collapse pressure (1.16-1.45 g/cm$^3$), followed by this new CPM (0.96-1.22 g/cm$^3$), the Mg-C criterion (0.93-1.17 g/cm$^3$), the MW-C criterion (0.84-1.12 g/cm$^3$), the ML criterion (0.88-1.11 g/cm$^3$), and the D-P criterion (0.82-1.17 g/cm$^3$). As shown in Figure 5 and Table 3, for the same well path under the SSF condition, the M-C criterion always gave the greatest collapse pressure (1.07-1.22 g/cm$^3$), followed by this new CPM (0.87-1.01 g/cm$^3$), the Mg-C criterion (0.85-0.97 g/cm$^3$), the D-P criterion (0.79-0.96 g/cm$^3$), the ML criterion (0.81-0.93 g/cm$^3$), and the MW-C criterion (0.75-0.89 g/cm$^3$). As shown in Figure 6 and Table 3, for the same well path under the RF condition, the M-C criterion always gave the greatest collapse pressure (0.99-1.26 g/cm$^3$), followed by this new CPM (0.80-1.05 g/cm$^3$), the Mg-C criterion (0.78-1.01 g/cm$^3$), the ML criterion (0.74-0.96 g/cm$^3$), the D-P criterion (0.71-1.03 g/cm$^3$), and the MW-C criterion (0.67-0.94 g/cm$^3$). On the whole, the different models predicted different EMW of collapse pressure. Under different stress regimes, the M-C criterion always gave the greatest EMW of collapse pressure owing to it ignoring the influence of the $\sigma_2$, followed by this new CPM and Mg-C criterion, but the other conventional models gave different results under different stress regimes, because the other conventional models involved the different influence of the $\sigma_2$ [54, 55], and this new CPM integrated the advantageous synergy of the five different criteria.

In addition, the best and worst well paths of wellbore stability of different models under different stress regimes are also listed in Table 4. The results indicated the following: (1) under the NF condition, only the D-P criterion predicted the most stable well path with the lowest collapse pressure as the vertical well, while the other conventional models and this new CPM predicted the most stable well path as the inclined well, and all of the conventional models and this new CPM predicted the worst stable well path with the greatest collapse pressure as the horizontal well. (2) Under

Table 5: Comparison between predicted EMW of collapse pressure and actual MW for different fields.

| No. | Field | Well type | Actual MW (g/cm$^3$) | M-C criterion | | New model | | Remarks |
|---|---|---|---|---|---|---|---|---|
| | | | | EMW (g/cm$^3$) | Error (%) | EMW (g/cm$^3$) | Error (%) | |
| 1 | YB area | Vertical | 1.15-1.20 | 1.46 | 21.7 | 1.31 | 9.2 | Underbalanced drilling, no wellbore collapse reports |
| 2 | CN area | Vertical | 1.30-1.40 | 1.82 | 30.0 | 1.48 | 5.7 | Breakout width 30-80°, no wellbore collapse reports |
| 3 | WY area | Vertical | 1.00-1.20 | 1.61 | 34.2 | 1.35 | 12.5 | Breakout width 40-90°, no wellbore collapse reports |
| 4 | TLM area | Inclined | 1.45-1.70 | 1.96 | 15.3 | 1.80 | 5.9 | MW = 1.45 wellbore collapse, MW > 1.70 wellbore stabilize |
| 5 | HS area | Horizontal | 1.17-1.28 | 1.40 | 9.4 | 1.31 | 2.3 | Breakout width 30-50°, no wellbore collapse reports |
| 6 | Average | | — | — | 22.1 | — | 7.1 | — |

the SSF condition, all of the conventional models and this new CPM predicted the most stable well path with the lowest collapse pressure as the horizontal well, and only the D-P criterion predicted the worst stable well path with the greatest collapse as the horizontal well, while the other conventional models and this new CPM predicted the worst stable well path as the vertical well. (3) Under the RF condition, all of the conventional models and this new CPM predicted the most stable well path with the lowest collapse pressure as the inclined well, and only the D-P criterion predicted the worst stable well path with the greatest collapse as the vertical well, while the other conventional models and this new CPM predicted the worst stable well path as the horizontal well. In other words, the selection of strength criterion may cause to different results of the best and worst well paths.

## 5. Field Cases

To further verify the accuracy of this new CPM, five kinds of typical oil and gas field data were collected [8, 57–60], the predicted EMW of collapse pressure and actual mud weight were predicted for different oil and gas fields using both conventional model (M-C criterion) and this new CPM, and the results are listed in Table 5, where three types of typical wells were encountered. It is clearly found that the M-C criterion always gave a much higher EMW of collapse pressure than this new CPM and the real MW used in oil and gas field. However, two types of typical wells, such as the vertical and horizontal wells in CN, WY, and HS area, were drilled successfully using a very low mud weight that is obviously lower than the predicted results of the conventional model, which means the conventional model is too conservative [8, 57, 58]. The EMW of collapse pressure predicted by this new CPM is much closer to the real mud weight used in real oil and gas field, which means that this new CPM is more reasonable and accurate. The prediction error of the conventional model ranges 9.4-34.2% with an average of 22.1%, while the prediction error of this new CPM ranges 2.3-12.5% with an average of 7.1%, and the average error has been lowered 15%, so this new CPM is more accurate than the conventional model.

## 6. Conclusions

An analytical model of WSA was proposed for inclined well by integrating the stress components and the advantageous synergy of the five different strength criteria, the predicted results among this new CPM and five conventional models were compared under three types of typical stress regimes, five kinds of typical oil and gas field data were collected to further verify this new CPM, and the following conclusions can be drawn:

(1) Under the NF condition, the M-C criterion always gave the greatest collapse pressure, followed by this new CPM and the Mg-C, MW-C, ML, and D-P criteria. The collapse pressure increased with borehole inclination along the $\sigma_H$ direction, while it decreased and then increased with borehole inclination along the $\sigma_h$ direction. The inclined well ($\psi \approx 42^\circ$) along the $\sigma_h$ direction had the best stability, while the horizontal well along the $\sigma_h$ direction had the worst stability, and the stability of horizontal and highly deviated wells parallel to the $\sigma_h$ direction was slightly better than that of $\sigma_H$ direction

(2) Under the SSF condition, the M-C criterion always gave the greatest collapse pressure, followed by this new CPM and the Mg-C, D-P, ML, and MW-C criteria. The collapse pressure decreased with borehole inclination along either the $\sigma_H$ direction or the $\sigma_h$ direction. The horizontal well deviated ~45° from the $\sigma_H$ direction had the best stability, while the vertical well had the worst stability, and the stability of horizontal and highly deviated wells parallel to the $\sigma_H$ direction was surely better than that of $\sigma_h$ direction

(3) Under the RF condition, the M-C criterion always gave the greatest collapse pressure, followed by this new CPM and the Mg-C, ML, D-P, and MW-C criteria. The collapse pressure slightly increased with borehole inclination along the $\sigma_h$ direction, while it decreased and then increased slightly with borehole inclination along the $\sigma_H$ direction. The inclined well

($\psi \approx 60\circ$) along the $\sigma_H$ direction had the best stability, while the horizontal well along the $\sigma_h$ direction had the worst stability, and the stability of horizontal and highly deviated wells parallel to the $\sigma_H$ direction was surely better than that of $\sigma_h$ direction

(4) The different models predicted different collapse pressure. Under different stress regimes, the M-C criterion always gave the greatest collapse pressure owing to it ignoring the influence of the $\sigma_2$, followed by these new CPM and Mg-C criteria, while the other conventional models gave different results under different stress regimes, because of the different influence of the $\sigma_2$, but this new CPM integrated the advantageous synergy of the five different criteria

(5) Under the NF condition, the most stable well path is the vertical for D-P criterion, while it is the inclined for the other models, and the worst stable well path is the horizontal for all models. Under the SSF condition, the most stable well path is the horizontal for all models, and the worst stable well path is the horizontal for D-P criterion, while it is the vertical for the other conventional and new models. Under the RF condition, the most stable well path is the inclined for all models, and the worst stable well path is the vertical for D-P criterion, while it is horizontal for the other conventional and new models. Thus, the selection of strength criterion may cause to different results of the best and worst well paths

(6) The prediction error of the conventional models was between 9.4% and 34.2% with an average of 22.1%, while the prediction error of this new CPM was between 2.3% and 12.5% with an average of 7.1%, and the average error has been lowered to 15%; thus, this new CPM is more accurate than the conventional model. In addition, this new CPM can be simplified as the conventional models by adjusting the weight coefficients. However, this new CPM ignored the influence of stress-seepage coupling, so the influence of time dependency of the stress and pore pressure is recommended to involve in the future

## Abbreviations

AHP: Analytic hierarchy process
CI: Consistency index
CPM: Collapse pressure model
CR: Consistency ratio
D-P: Drucker-Prager
EMW: Equivalent mud weight
EPS: Effective principal stress
H-B: Hoek-Brown
HP/HT: High pressure/high temperature
M-C: Mohr-Coulomb
Mg-C: Mogi-Coulomb
ML: Modified Lade
MW: Mud weight
MW-C: Modified Wiebols-Cook
NF: Normal fault
RF: Reverse fault
SSF: Strike-slip fault
SMWW: Safe mud weight window
TVD: True vertical depth
UCS: Uniaxial compressive strength
WSA: Wellbore stability analysis.

## Data Availability

The data presented in this study are available on request from the corresponding author.

## Conflicts of Interest

The authors declare no conflict of interest.

## Acknowledgments

This research was funded by the Nanchong-SWPU Science and Technology Strategic Cooperation Foundation (Grant No. SXHZ033) and the Sichuan Science and Technology Program (Grant No. 2020JDJQ0055).

## References

[1] Z. Jin, J. Zhang, and X. Tang, "Unconventional natural gas accumulation system," *Natural Gas Industry B*, vol. 9, no. 1, pp. 9–19, 2022.

[2] F. Zhang, L. Cui, M. An, D. Elsworth, and C. He, "Frictional stability of Longmaxi shale gouges and its implication for deep seismic potential in the southeastern Sichuan Basin," *Deep Underground Science and Engineering*, vol. 1, no. 1, pp. 3–14, 2022.

[3] D. Guo, Y. Kang, Z. Wang, Y. Zhao, and S. Li, "Optimization of fracturing parameters for tight oil production based on genetic algorithm," *Petroleum*, vol. 8, no. 2, pp. 252–263, 2022.

[4] S. Chen, C. Zhang, X. Li, Y. Zhang, and X. Wang, "Simulation of methane adsorption in diverse organic pores in shale reservoirs with multi-period geological evolution," *International Journal of Coal Science & Technology*, vol. 8, no. 5, pp. 844–855, 2021.

[5] X. Pang, H. Li, and H. Pang, "Exploring the mysteries of deep oil and gas formation in the South China Sea to guide Palaeocene exploration in the Pearl River Mouth Basin," *Advances in Geo-Energy Research*, vol. 6, no. 5, pp. 361-362, 2022.

[6] T. Ma, P. Chen, and J. Zhao, "Overview on vertical and directional drilling technologies for the exploration and exploitation of deep petroleum resources," *Geomechanics and Geophysics for Geo-Energy and Geo-Resources*, vol. 2, no. 4, pp. 365–395, 2016.

[7] T. Ma, J. Liu, J. Fu, and B. Wu, "Drilling and completion technologies of coalbed methane exploitation: an overview," *International Journal of Coal Science & Technology*, vol. 9, no. 1, p. 68, 2022.

[8] T. Ma, P. Chen, C. Yang, and J. Zhao, "Wellbore stability analysis and well path optimization based on the breakout width model and Mogi-Coulomb criterion," *Journal of Petroleum Science and Engineering*, vol. 135, pp. 678–701, 2015.

[9] Y. Liu, T. Ma, P. Chen, and C. Yang, "Method and apparatus for monitoring of downhole dynamic drag and torque of

drill-string in horizontal wells," *Journal of Petroleum Science and Engineering*, vol. 164, pp. 320–332, 2018.

[10] T. Yan, J. Y. Qu, X. F. Sun, W. Li, Y. Chen, and Q. B. Hu, "A novel predictive model of drag coefficient and settling velocity of drill cuttings in non-Newtonian drilling fluids," *Petroleum Science*, vol. 18, no. 6, pp. 1729–1738, 2021.

[11] L. Yuan, S. Jiangang, N. Minghu, P. Chi, and W. Yingjie, "Drill string dynamic characteristics simulation for the ultra-deep well drilling on the south margins of Junggar Basin," *Petroleum*, 2021.

[12] D. Gao, "Some research advances in well engineering technology for unconventional hydrocarbon," *Natural Gas Industry B*, vol. 9, no. 1, pp. 41–50, 2022.

[13] Q. Zhang, S. Qin, Z. Rao, B. Tian, and K. Zuo, "Key drilling technologies in extended-reach well M with ultra-high HD/VD ratio in the South China Sea," *Petroleum Drilling Techniques*, vol. 49, no. 5, pp. 19–25, 2021.

[14] C. Yang and J. Liu, "Petroleum rock mechanics: an area worthy of focus in geo-energy research," *Advances in Geo-Energy Research*, vol. 5, no. 4, pp. 351-352, 2021.

[15] Y. Li, Y.-F. Cheng, C.-L. Yan, Z.-Y. Wang, and L.-F. Song, "Effects of creep characteristics of natural gas hydrate-bearing sediments on wellbore stability," *Petroleum Science*, vol. 19, no. 1, pp. 220–233, 2022.

[16] H. Yu, J. Chen, D. Li, H. Yi, Y. Zeng, and X. Li, "Study of a rock burst tendency identification method in deep and ultra-deep hard/brittle formations," *Petroleum Science Bulletin*, vol. 6, no. 3, pp. 441–450, 2021.

[17] Y. Kang, M. Yu, S. Z. Miska, and N. Takach, "Wellbore stability: a critical review and introduction to DEM," in *SPE Annual Technical Conference and Exhibition*, New Orleans, Louisiana, October 2009.

[18] M. Faraji, A. Rezagholilou, M. Ghanavati, A. Kadkhodaie, and D. A. Wood, "Breakouts derived from image logs aid the estimation of maximum horizontal stress: a case study from Perth Basin, Western Australia," *Advances in Geo-Energy Research*, vol. 5, no. 1, pp. 8–24, 2021.

[19] J. J. Zhang, *Applied Petroleum Geomechanics*, Gulf Professional Publishing, Cambridge, MA, United States, 2019.

[20] E. Fjaer, R. M. Holt, P. Horsrud, and A. M. Raaen, *Petroleum Related Rock Mechanics*, Elsevier, Amsterdam, The Netherlands, 2nd edition, 2008.

[21] M. Chen, Y. Jin, and G. Q. Zhang, *Petroleum Engineering Rock Mechanics*, Science Press, Beijing, China, 2008.

[22] T. Ma, H. Wang, Y. Liu, Y. Shi, and P. G. Ranjith, "Fracture-initiation pressure model of inclined wells in transversely isotropic formation with anisotropic tensile strength," *International Journal of Rock Mechanics and Mining Sciences*, vol. 159, article 105235, 2022.

[23] T. Ma, J. Huang, L. Jia, Y. Liu, Y. Qiu, and Y. Zhang, "Wellbore stability analysis for arbitrary inclined well in anisotropic formations," *IOP Conference Series: Earth and Environmental Science*, vol. 570, no. 6, article 062032, 2020.

[24] Y. Deng, S. He, X. Deng, Y. Peng, S. He, and M. Tang, "Study on wellbore instability of bedded shale gas horizontal wells under chemo-mechanical coupling," *Petroleum Drilling Techniques*, vol. 48, no. 1, pp. 26–33, 2020.

[25] Z. Xu, Y. Jin, and X. Liu, "Study of inhibition performance and the mechanism of action of alkyl glucoside quaternary ammonium salt as a new shale inhibitor," *Petroleum Science Bulletin*, vol. 5, no. 1, pp. 67–77, 2020.

[26] T. Ma, T. Tang, P. Chen, and C. Yang, "Uncertainty evaluation of safe mud weight window utilizing the reliability assessment method," *Energies*, vol. 12, no. 5, p. 942, 2019.

[27] Z. Qian, "Development and testing of high temperature resistant composite salt drilling fluid system," *Chinese Petroleum and Natural Gas Research*, vol. 1, no. 1, pp. 1–8, 2022.

[28] R. Gholami, A. Raza, M. Rabiei et al., "An approach to improve wellbore stability in active shale formations using nanomaterials," *Petroleum*, vol. 7, no. 1, pp. 24–32, 2021.

[29] T. Ma, Y. Zhang, Y. Qiu, Y. Liu, and Z. Li, "Effect of parameter correlation on risk analysis of wellbore instability in deep igneous formations," *Journal of Petroleum Science and Engineering*, vol. 208, article 109521, 2022.

[30] T. Ma, Y. Qiu, Y. Zhang, and Y. Liu, "Numerical simulation of progressive sand production of open-hole completion borehole in heterogeneous igneous formation," *International Journal of Rock Mechanics and Mining Sciences*, vol. 150, article 105030, 2022.

[31] C. L. Yan, L. F. Dong, K. Zhao et al., "Time-dependent borehole stability in hard-brittle shale," *Petroleum Science*, vol. 19, no. 2, pp. 663–677, 2022.

[32] Z. Fan and R. Parashar, "Analytical solutions for a wellbore subjected to a non-isothermal fluid flux: implications for optimizing injection rates, fracture reactivation, and EGS hydraulic stimulation," *Rock Mechanics and Rock Engineering*, vol. 52, no. 11, pp. 4715–4729, 2019.

[33] Z. Fan, P. Eichhubl, and P. Newell, "Basement fault reactivation by fluid injection into sedimentary reservoirs: poroelastic effects," *Journal of Geophysical Research: Solid Earth*, vol. 124, no. 7, pp. 7354–7369, 2019.

[34] L. Chen, D. Zhao, J. Yin, M. Wang, and B. Liu, "Effect of geostress field on critical collapse pressure of bottom hole in horizontal well," *Natural Gas and Oil*, vol. 30, no. 2, pp. 42–44, 2012.

[35] T. Ma and P. Chen, "A wellbore stability analysis model with chemical-mechanical coupling for shale gas reservoirs," *Journal of Natural Gas Science and Engineering*, vol. 26, pp. 72–98, 2015.

[36] T. Ma, P. Chen, Q. Zhang, and J. Zhao, "A novel collapse pressure model with mechanical-chemical coupling in shale gas formations with multi-weakness planes," *Journal of Natural Gas Science and Engineering*, vol. 36, pp. 1151–1177, 2016.

[37] T. Ma, J. Huang, Z. Li, Y. Shi, L. Jia, and C. Zhong, "Influence of drill-string lateral collision on wellbore stability of a horizontal well," *Advances in Mechanical Engineering*, vol. 14, no. 6, 2022.

[38] W. B. Bradley, "Failure of inclined boreholes," *Journal of Energy Resources Technology*, vol. 101, no. 4, pp. 232–239, 1979.

[39] R. T. Ewy, "Wellbore-stability predictions by use of a modified Lade criterion," *SPE Drilling & Completion*, vol. 14, no. 2, pp. 85–91, 1999.

[40] L. B. Colmenares and M. D. Zoback, "A statistical evaluation of intact rock failure criteria constrained by polyaxial test data for five different rocks," *International Journal of Rock Mechanics and Mining Sciences*, vol. 39, no. 6, pp. 695–729, 2002.

[41] A. M. Al-Ajmi and R. W. Zimmerman, "Relation between the Mogi and the Coulomb failure criteria," *International Journal of Rock Mechanics and Mining Sciences*, vol. 42, no. 3, pp. 431–439, 2005.

[42] A. M. Al-Ajmi and R. W. Zimmerman, "Stability analysis of vertical boreholes using the Mogi-Coulomb failure criterion,"

*International Journal of Rock Mechanics and Mining Sciences*, vol. 43, no. 8, pp. 1200–1211, 2006.

[43] A. Singh, K. S. Rao, and R. Ayothiraman, "An analytical solution to wellbore stability using Mogi-Coulomb failure criterion," *Journal of Rock Mechanics and Geotechnical Engineering*, vol. 11, no. 6, pp. 1211–1230, 2019.

[44] X. Yang, X. Shi, Y. Meng, and X. Xie, "Wellbore stability analysis of layered shale based on the modified Mogi-Coulomb criterion," *Petroleum*, vol. 6, no. 3, pp. 246–252, 2020.

[45] L. Zhang, P. Cao, and K. C. Radha, "Evaluation of rock strength criteria for wellbore stability analysis," *International Journal of Rock Mechanics and Mining Sciences*, vol. 47, no. 8, pp. 1304–1316, 2010.

[46] S. Maleki, R. Gholami, V. Rasouli, A. Moradzadeh, R. G. Riabi, and F. Sadaghzadeh, "Comparison of different failure criteria in prediction of safe mud weigh window in drilling practice," *Earth-Science Reviews*, vol. 136, pp. 36–58, 2014.

[47] M. Chabook, A. Al-Ajmi, and V. Isaev, "The role of rock strength criteria in wellbore stability and trajectory optimization," *International Journal of Rock Mechanics and Mining Sciences*, vol. 80, pp. 373–378, 2015.

[48] A. Elyasi and K. Goshtasbi, "Using different rock failure criteria in wellbore stability analysis," *Geomechanics for Energy and the Environment*, vol. 2, pp. 15–21, 2015.

[49] T. Ma, Z. Yang, and P. Chen, "Wellbore stability analysis of fractured formations based on Hoek-Brown failure criterion," *International Journal of Oil, Gas and Coal Technology*, vol. 17, no. 2, pp. 143–171, 2018.

[50] M. Meng, P. Chen, and R. Ren, "Statistic evaluation of failure criteria in wellbore stability with temperature effects," *Fuel*, vol. 252, pp. 730–752, 2019.

[51] M. Aslannezhad, A. Keshavarz, and A. Kalantariasl, "Evaluation of mechanical, chemical, and thermal effects on wellbore stability using different rock failure criteria," *Journal of Natural Gas Science and Engineering*, vol. 78, article 103276, 2020.

[52] T. Wang, Y. Liu, M. Cai, W. Zhao, P. G. Ranjith, and M. Liu, "Optimization of rock failure criteria under different fault mechanisms and borehole trajectories," *Geomechanics and Geophysics for Geo-Energy and Geo-Resources*, vol. 8, no. 4, p. 127, 2022.

[53] L. Zhang, Y. Bian, S. Zhang, and Y. Yan, "A new analytical model to evaluate uncertainty of wellbore collapse pressure based on advantageous synergies of different strength criteria," *Rock Mechanics and Rock Engineering*, vol. 52, no. 8, pp. 2649–2664, 2019.

[54] X. Wang, Z. Xu, Y. Sun, J. Zheng, C. Zhang, and Z. Duan, "Construction of multi-factor identification model for real-time monitoring and early warning of mine water inrush," *International Journal of Mining Science and Technology*, vol. 31, no. 5, pp. 853–866, 2021.

[55] Z. Song, Z. Zhang, P. G. Ranjith, W. Zhao, and C. Liu, "Experimental study on the influence of hydrostatic stress on the Lode angle effect of porous rock," *International Journal of Mining Science and Technology*, vol. 32, no. 4, pp. 727–735, 2022.

[56] A. M. Abdulaziz, H. L. Abdulridha, A. S. A. Dahab, S. Alhussainy, and A. K. Abbas, "3D mechanical earth model for optimized wellbore stability, a case study from south of Iraq," *Journal of Petroleum Exploration and Production Technology*, vol. 11, no. 9, pp. 3409–3420, 2021.

[57] T. Ma, N. Peng, T. Tang, and Y. Wang, "Wellbore stability analysis by using a risk-controlled method," in *52nd U.S. Rock Mechanics Geomechanics Symposium*, Seattle, Washington, USA, June 2018.

[58] T. Ma, T. Tang, N. Peng, Y. Wang, and Z. Guo, "Use of risk-controlled model for predicting collapse pressure of vertical and inclined wells," in *International Conference on Geomechanics, Geo-energy and Geo-resources 2018*, Chengdu, China, September 2018.

[59] L. Qin, Y. Li, H. Wu, Y. Zhang, S. Li, and G. Xie, "Stress modeling and well stability of well Yuanba 11 in Yuanba area in northeastern Sichuan Basin," *Science & Technology Review*, vol. 30, no. 34, pp. 45–50, 2012.

[60] H. Wen, M. Chen, Y. Jin et al., "A chemo-mechanical coupling model of deviated borehole stability in hard brittle shale," *Petroleum Exploration and Development*, vol. 41, no. 6, pp. 817–823, 2014.